Turun yliopisto
University of Turku

Manufacture and Analysis of N-type Semiconductor Layer and Perovskite Layer in Hybrid Perovskite Solar Cell

Master thesis

Peng Bo

The originality of this thesis has been checked in accordance with the University of Turku quality assurance system using the Turnitin OriginalityCheck service.

Preface

This thesis work is carried out at the Laboratory of Material Chemistry Research Group, University of Turku, Turku, Finland.

I would like to give my thanks to all the group members in the material chemistry group and friends who worked in the same labs with me. Everyone offered me much help during the experimental and writing progress of this thesis. When I started the program, barely can I even think about how to carry out a scientific research. They are the sources of my inspiration and motivation.

When looking back at my master life, I am truly blessed to be accepted by the University of Turku and to meet so many wonderful people here. Carita Kvarnström, Pia Damlin, and Mikko Salomäki, these three outstanding scientists taught me much valuable knowledge and skills. They are always willing to offer help whenever I need it and have given me many advices. I have learned so much from these enthusiastic and experienced scientists not only about this program but the general thinking of all scientific researches.

Rahul Yewale, Milla Suominen, Nianxing Wang, and other good friends and colleagues provided me countless times of help on my academic research as well as personal life in Turku. Special thanks to Esa-Pekka Mattila, who is a kind and enthusiastic college I worked with. He is very generous to offer me his experimental products so I can have this thesis. Also special thanks to Uda lab in Tohoku University Japan, thanks for the valuable study experience and knowledge.

From the bottom of my heart, I am really grateful to all the help and advices received from all my friends and family. Your passion of science and kindness of heart supported me all the way through.

Peng Bo
2019, Turku

Abstract

This thesis work describes the experiments about building the first two layers of MethylAmmonium Lead Iodide perovskite solar cell and the conclusions made upon it. Different methods were used to get the optimized results. Obtained films were analyzed qualitatively by IR and Raman spectroscopy. Electrochemistry and spin coating are introduced into the experiments and showed a good result. Repeatable and stable layers are able to be obtained by detailed manufacture methods.

Key words: PEDOT: PSS, Perovskite, Spin Coating, Electroplating

Abbreviations

PHJ= Planar Heterojunction

PEC= Power Conversion Efficiency

HTL= Hole Transporting Layer

ETL= Electron Transporting Layer

PCBM= [6,6]-phenyl-C61-butyric acid methyl ester

PEDOT: PSS= Poly(3,4-ethylenedioxythiophene) Polystyrene Sulfonate

MAPI= MethylAmmonium Lead Iodide

DMSO= Dimethyl sulfoxide

DMF= Dimethylformamide

GBL= Gamma-Butyrolactone

FTO= Fluorine-doped Tin Oxide

BBL= Poly(benzimidazobenzophenanthroline)

MAI= MethylAmmonium Iodide (CH_3NH_3I)

HI= Hydrogen Iodide

Zonyl= $(C_2H_4O)_x(CF_2)_yC_2H_5FO$

Contents

1.Introduction

1.1 Solar Cells and Perovskite-based Solar Cells

Decades ago, people started to focus on sustainable lifestyle rather than just consume the energy source from nature. Green energy became the popular topic that many scientists devote their efforts in. There are many kinds of green energies, for example, wind energy, hydro power, geothermal energy, tidal energy and solar energy. Those energy sources are more sustainable and environmental-friendly comparing to traditional energy, like coal. Researches related are mainly focus on the conversion and storage of green energies. Solar cell is one of the most studied. Solar cell is an invention takes advantage of the sunlight and convert it to electricity, heat and other forms of energies which can be used. Tradition solar cells are silicon-based products, the structure of it is called planar heterojunction (PHJ) structure.

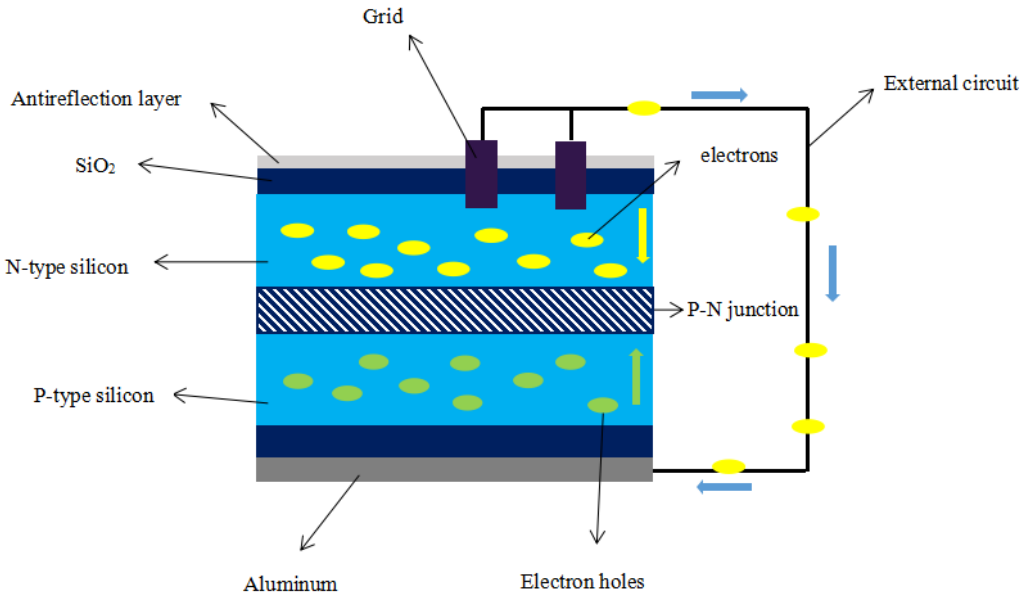

Fig. 1-1 Mechanism of silicon-based solar cell.

Fig.1-1 shows the working function of a silicon-based solar cell. The cell is consisting of different layers of materials including antireflection layer, silica layer, metal layer, p type and n type semiconductor layer. The critical parts are n- and p-type semiconductor layers (n- and p-type silicon in this case) which are also called impurity semiconductors. These can be obtained by doping certain elements in the base material and thereout manipulating the number of electrons in them. Doping atoms with more electrons

(Donor) than the base material makes the impurity semiconductor an n-type semiconductor. While it is named as a p-type semiconductor when doping with atoms with fewer electrons (Acceptor) than base material. Comparing to silicon, we consider that the n-type silicon in the cell has more electrons while the p-type silicon owns more vacant sites (holes) for the electrons to be in. The interface of two types of semiconductors is called p-n junction and it is with can be used to make a diode and a bipolar transistor.

According to Fig.1-1, the mechanism of silicon-based solar cell can be described as following: Hitting by photons, electrons in n-type silicon excite from ground state and become active. Some excited electrons give out energy, such as heat, and go back to the ground state; others travel through the semiconductor and reach the p-n junction to unite with the holes in p-type silicon thus to be at least energy state. Because of the movement of electrons, the n-type silicon is slightly positive changed while p-type silicon is a little bit negative charged. A potential difference has been generated by this phenomenon. An external electric circuit is connected. Due to the potential difference, electrons from n-type silicon start to flow to the p-type silicon via the circuit. The current is collected and converted to electricity.

Traditional silicon-based solar cells have rigid manufacturing registrations and high budget to start the business. The single silicon crystal must hold a purity of not less than 99.999% and the assembling environment must be dust free. The attempt to obtain a better solution never stopped. Different kinds of solar cells based on various materials and structures have been studied for decades.

Solar cells can be designed as mono-junction structure and multi-junction structurer. Multi-junction solar cells are solar cells with more than one p-n junctions. This structure makes the cell able to absorb different wavelength of sunlight and generate much energy. Thus, it has the highest efficiency. However, the higher expenditure makes it extremely untoward to start a business from. Mono-junction solar cell, on the other side, has only one p-n junction which generate less energy than multi-junction cells. The silicon-based cell is one of the most studied mono-junction cells. Perovskite solar cells have a really close efficiency comparing to silicon based solar cell. Yet, lower expense and much simpler manufacturing techniques make perovskite solar cell more appealing than it.

Years ago, scientists noticed that perovskite have a good potential to harvest energy from sun for its high diffusion length, broad light absorption range as well as a high coefficient of absorption [1-4], and the study of perovskite solar cell begins since. The first attempt of building a solar cell using perovskites on TiO_2 was reported in 2009. With a power conversion efficiency (PCE) of 3.8%, the group succeeded. [5] After years of research, the PCE of perovskite-based cell has reached over 20% which gives the cell a promising future.

Perovskite solar cells have two types of structures: meso-superstructured and planar heterojunction. [6-9] Although they share a common structure like a sandwich, they are not the same as silicon-based one. Perovskite replaces p-n junction comparing to silicon solar cell. Fig.1-2 shows the structure of meso-superstructured perovskite solar cell. For this kind, perovskite is infiltrated into a layer of metal oxide scaffold. In order to get this product, high temperature sintering is often required.

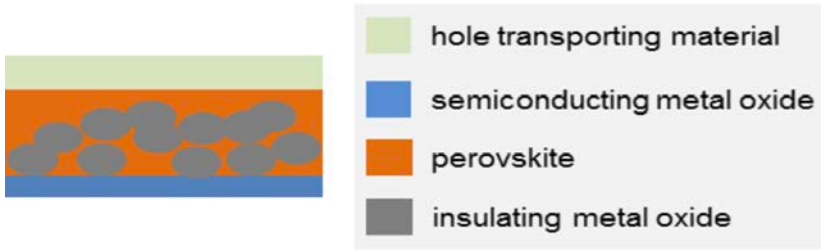

Fig.1-2 Meso-superstructured perovskite solar cell. [10]

On the other hand, planar heterojunction perovskite solar cell is more popular because it concurs the problem with high temperature sintering by having a perovskite layer between hole transporting layer (HTL) and electron transporting layer (ETL).

The structure of PHJ perovskite solar cell is shown below in Fig.1-3.

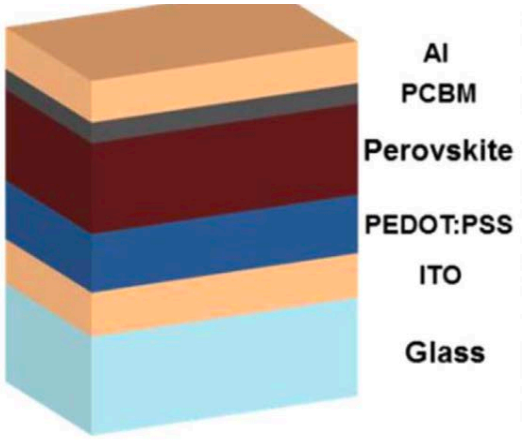

Fig.1-3 Structure of planer heterojunction perovskite solar cell. [11]

As mentioned, comparing to silicon-based solar cell, it has a different mechanism. In this unit, perovskite is the part that interact with photons and generate free electrons and simultaneously electron holes. Generated free electrons travels to n-type semiconductor which is PEDOT: PSS in this figure and electron holes travels to p-type semiconductor which is PCBM is this case. The metal layer, p-type semiconductor layer and perovskite layer work together as a cathode while the rest together work as an anode. By creating an external circuit, the potential difference shows in two "electrodes" and thus electricity can be obtained by manipulating the current flowing though the circuit.

PEDOT:PSS (Poly(3,4-ethylenedioxythiophene) Polystyrene Sulfonate) is a kind of polymer mixture of 2 kinds of isomers. One is negative charged sodium polystyrene sulfonate and the other is positive charged Poly(3,4-ethylenedioxythiophene). It is a conducting polymer with high conductivity, high light transmittance and relatively high stability. PEDOT:PSS can be used as n-type material in perovskite solar cell. Fig 1-4 shows the structure of PEDOT:PSS.[39]

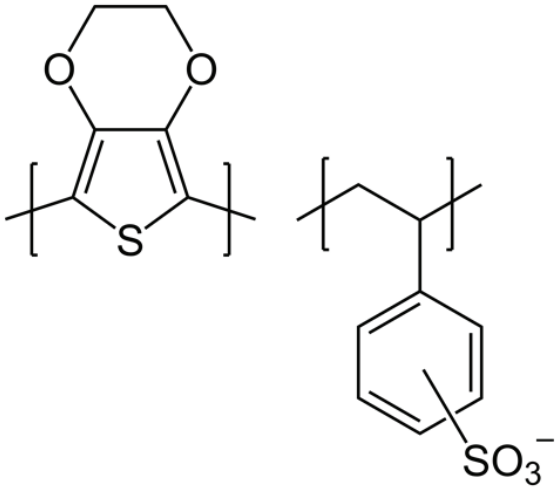

Fig 1-4 Structure of PEDOT:PSS.

Manufacturing techniques of perovskite solar cells are rather simple comparing to those of others. The main methods used for planar heterojunction perovskite cells are spin coating and electroplating which will be explained in the following context.

1.2 Perovskites

Perovskite originally means the calcium titanium oxide mineral composed of calcium titanate ($CaTiO_3$). It is named after a Russian mineralogist Lev Perovski (1792–1856).

In 1926, a Norwegian mineralogist, Victor Goldschmidt, discovered the perovskite crystal structure in his work on tolerance factors. [12] In 1945, Helen Dick Megaw published the crystal structure of perovskite from X-ray diffraction data on barium titanite. [13] Nowadays, people use the term perovskite to represent material with similar cubic Pm3m framework structure of composition ABX_3.

1.2.1 Structure of Perovskite

Fig.1-5 shows the illustration of ABX_3 crystal structure of perovskite. In the cubic unit, the red spheres represent negatively charged X atoms. The black dot in the center of the cubic stands for B atom which are normally positively-charged smaller metal cations. Blue balls in the corner of the cubic are A atoms. A atoms are usually larger-sized metal cations and they are often selected to neutralize the total charge.

A atom is commonly coordinated with 12 X anions atoms while B atom is coordinated with 6 X anions atoms. Extending the cubic to multiple units, it can be seen that BX_6 octahedra are corner-connected to form an octahedron. The hinged octahedra allow for wide adjustment of the B-X-B bond angle. [14]

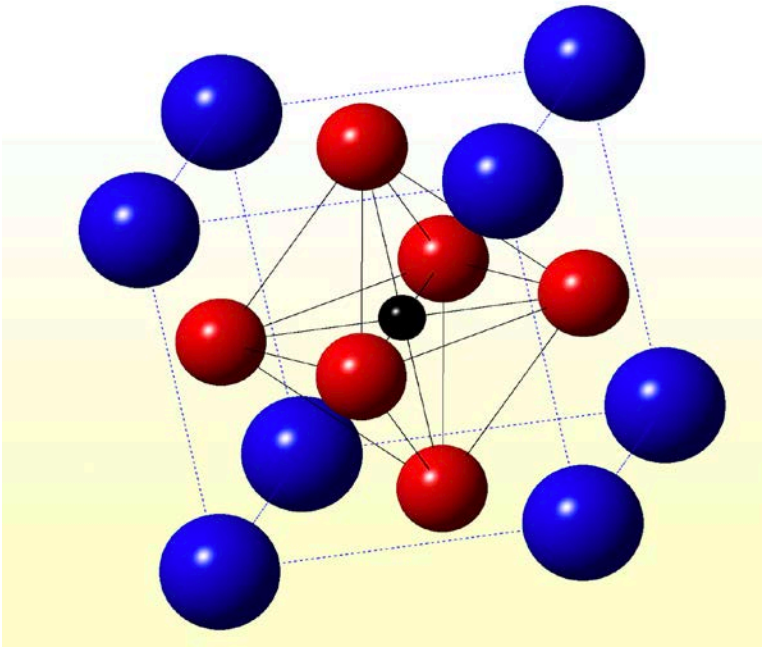

Fig. 1-5 Structure of ABX_3 crystal.

For solar energy harvesting, hybrid perovskite is the most popular one among its kind. By exchanging A atoms to organic positively charged groups, hybrid perovskite can be prepared. Methylammonium lead iodide ($CH_3NH_3PbI_3$) and its derivatives are currently being studied and wildly used in many different research groups.

$MAPbI_3$ have a relatively small forbidden bandwidth (energy gap) around 1.5eV [15] which makes it promising in solar cell applications. Although it is not as ideal as silicon who has a band gap energy of 1.1eV, the simplicity of manufacture makes perovskite more attractive,

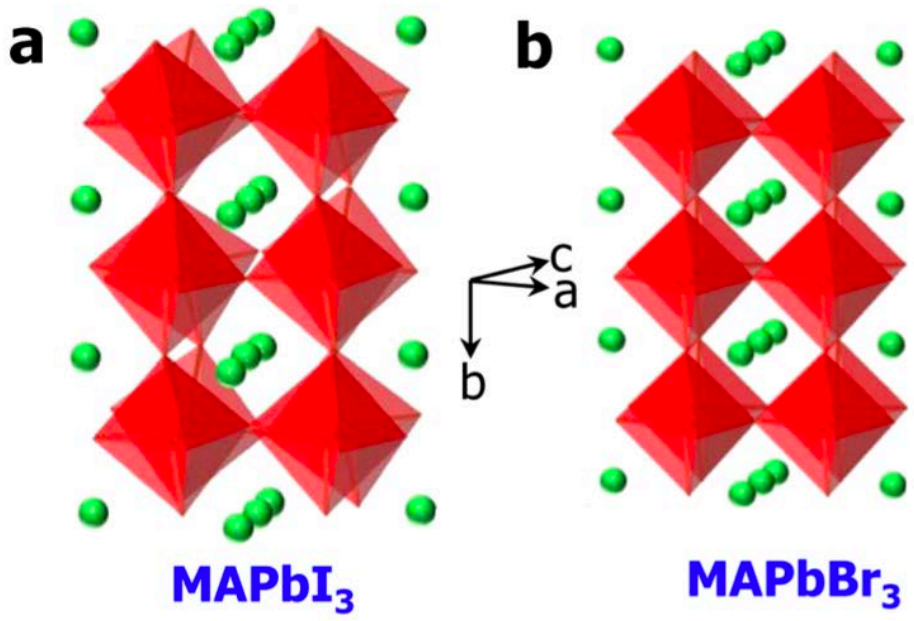

Fig.1-6, (a) Distorted perovskite structure of $MAPbI_3$ at room temperature; (b) Cubic perovskite structure of $MaPbBr_3$ at room temperature. [15]

By replacing the iodide to other halogen elements, different kinds of hybrids perovskite can be made. Fig.1-6 shows crystal structures of perovskite with Br and I as x-site atom respectively. With the ionic radius of B atoms in ABX_3 structure increasing, BX_6 octahedrons start to distort from their regular positions. Iodide have a larger ionic radius (2.2Å) with six-fold coordination than bromide (1.96Å), thus the BX_6 octahedrons in $MAPbI_3$ are distorted while those in $MAPbBr_3$ are not. Relatively more stable structure gives $MAPbBr_3$ a higher band gap energy (2.2eV).

By adjusting the ratio of iodide to bromide in perovskite $MAPb(I_xBr_{1-x})_3$, the efficiency change of solar cell products can be observed. When X in $MAPb(I_xBr_{1-x})_3$ rising from 0 to 0.2, the efficiency of corresponding solar cell increases. However, when X is larger than 0.2, the efficiency starts to drop. Also, under unity environmental conditions, the most stable perovskite is obtained when x equals 0.2. The change of energy band gap of $MAPb(I_xBr_{1-x})_3$ also shows a linear relationship with X.[15]

1.2.2 Hybrid Perovskite

One of the main obstacles one may encounter when working with hybrid perovskite is the easy-decomposing feature. It is crucial for researchers whoever working on this material to find a way to solve the problem.

The initiations of hybrid perovskite decomposition are mainly moisture, heat and light. Although they all contribute to the degradation of hybrid perovskite, water is the most critical cause. The instability of hybrid perovskite is mainly because of its low crystal formation energy and hydroscopic nature. [16, 22] Under ambient conditions, the decomposing processes is shown below [17]:

$$4MAPI + 8H_2O \rightarrow (CH_3NH_3)_4PbI_6 \cdot 2H_2O + 3Pb(OH)_2 + 6HI \uparrow \quad (1)$$

$$(CH_3NH_3)_4PbI_6 \cdot 2H_2O \rightarrow (CH_3NH_3)_x PbI_{2+x} + (4-x)CH_3NH_2 \uparrow + (4-x)HI + 2H_2O \quad (2)$$

$$2(CH_3NH_3)_x PbI_{2+x} + 2CO_2 + O_2 \rightarrow PbCO3 + 2I_2 \uparrow + 2x\, CH_3NH_2 \uparrow 2xHI \uparrow \quad (3)$$

$$2(CH_3NH_3)_x PbI_{2+x} + H_2O + 1/2\, O_2 \rightarrow Pb(OH)_2 + I_2 \uparrow + xHI \uparrow + xCH_3NH_2 \uparrow \quad (4)$$

$$Pb(OH)_2 \rightarrow PbO + H_2O \quad (5)$$

These degeneration processes are mainly about the transformation of low-band-gap MAPI to relatively high band gap hydrate materials. Exposing to light might accelerate the decomposing process. Equation (1) is the hydration process of MAPI and equation (2) is the dehydration of the product of equation (1) [18]. Transient phase product $(PbI_{2+x})^{x-}$ is generated because the hydrate product is only stable in highly humid environment. That means in ambient conditions, $(CH_3NH_3)_4PbI_6 \cdot 2H_2O$ is unstable and can easily react. Following equation (3) to equation (5), MAPI would finally degenerate to other lead products. This degradation procedure is followed by a color change from black to transparent owing to the formation of hydrated perovskite phases. [19-21]

More precisely, during [24] the reaction of equation (1), there is another side reaction happening. MAPI absorbs water and forms MAPI $\cdot$ H_2O, this process is reversible. By drying process, MAPI $\cdot$ H_2O will lose water attached, and become pristine material again. [21,23] However, the reverse reaction is with a limitation of within 5-10% area of perovskite degradation [16]. Interestingly, sometimes water can actually enhance the efficiency of perovskite solar cells [36-37], but for maintaining the efficiency of the system, it should be prevented.

Current researches about the optimization of the stability of hybrid perovskite and the efficiency of its solar cell products can be concluded into three different manipulations. First, better control on the morphology of the perovskite film; second, modifications upon the reactants of perovskite; third, carefully choose of solvent treatment.

For first method, many diverse techniques were used to control the morphology of perovskite film. For MAPI, the size of crystals has a huge influence on the sensitivity to moisture. Large crystal size makes perovskite more stable. It is because of the place where water molecules get in and start decomposing the material which is the crystal grain boundaries. Fig.1-7 illustrates how perovskite decompose from the grain boundaries. [16] The decomposition goes along the in-plain direction and it is initiated at the grain boundaries. Between two crystal grains, exists an amorphous intergranular layer with a thickness around 5nm [16] and it is that layer who makes water quickly diffused into the film of perovskite. The grain boundaries can be significantly adjusted by many high-tech film making techniques. Thus, the efficiency of perovskite solar cell can be improved. [30-32]

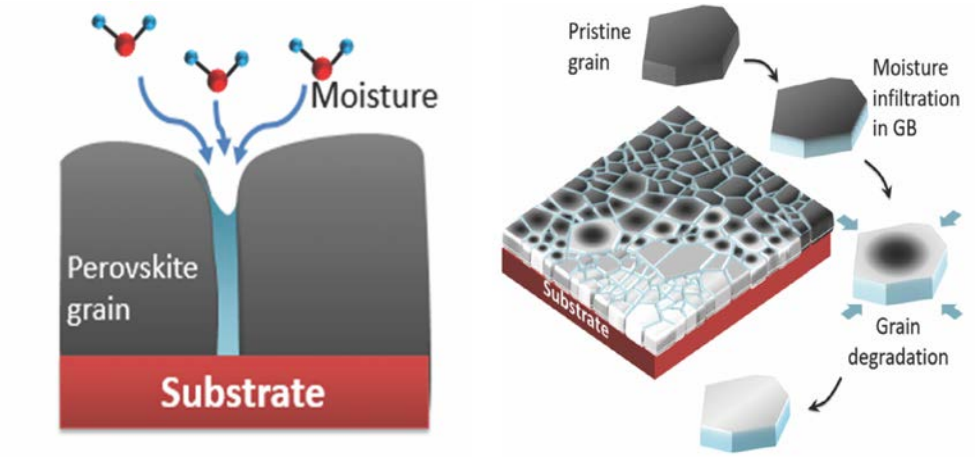

Fig.1-7 Illustration of how perovskite decompose, GB is short for grain boundaries.

Sintering for different time after the formation of perovskite films can provide various grain sizes. During the process, many water-sensitive $CH_3NH_2^+$ ions on surface of crystal grains can be eliminated. Principally, larger grain size makes it more durable to humidity.

For second approach, an example has been given in 1.2.1 Structure of Perovskite. By adjusting the X atoms in ABX_3 structure, the efficiency can be improved. It is also reported that MAPI is more sensitive to moisture than $MAPbBr_3$. [24] A atoms are also changed in different ways to test the outcomes of perovskite. By increasing the degree

of methyl-fluorination, the dipole moment of the perovskite crystal is greatly changed as shown in fig.1-8. [25] When preparing MAPI, different ratio of MAI and PbI_2 may lead to dramatically different results. [26]

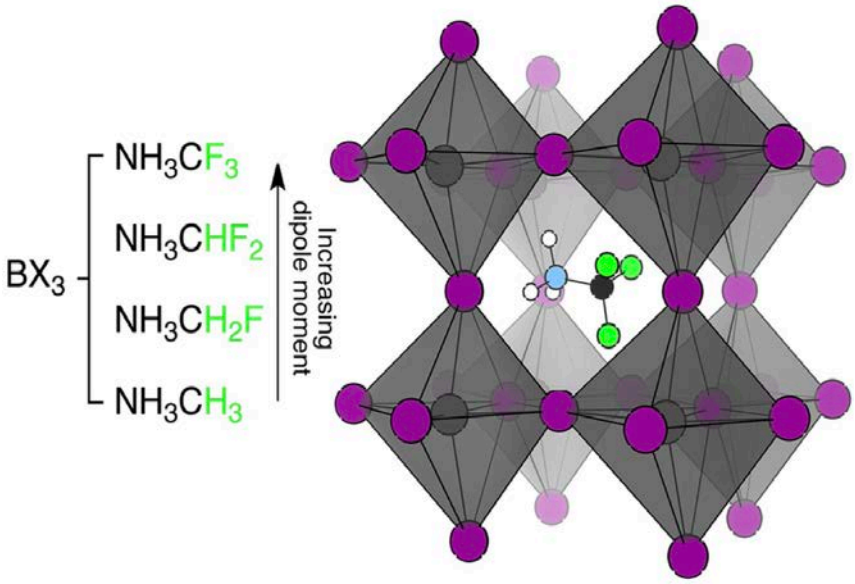

Fig.1-8. Dipole moment is increasing when replacing H atom to F atom and it shows an increasing trend.

The last manipulation is based on the fact that most of the methods for perovskite films today are solvent involved. Using a solvent which might react in the procedure of perovskite forming would surely increase the complexity of the experiment, but also gives more possibility to enhance the procedure of perovskite film formation by interaction with the reactants. DMSO, DMF, and GBL are common solvent in perovskite film formation, they are active as coordinating ligands that influence the solution chemistry and the behaviors of films. [26-28] The character of perovskite can also be tuned and influenced by adding chloride ions. [29] Although the mechanism is still not fully understood, it shows a great prospect.

1.3 Spin Coating and Electrodeposition

Main manufacture methods utilized in this thesis are spin coating and electrodeposition. They are both very simple and easy to master. Easy-producing character makes perovskite solar cells ~~are~~ very competitive nowadays.

1.3.1 Spin coating

Spin coating refers to a technique that deposit a thin layer of materials onto a flat substrate. The main mechanism of this technique is using the centrifugal force to make the coating material on top of the spinning substrate spread all over the surface to from a film. The equipment for spin coating is called a spinner or a spin coater.

On the working platform of spin coater, there is a sink like structure which allows substrate firmly attached to spin coater. Spin speed and spin time can be adjusted by equipment. The solution for coating is put on top of the substrate by pipette.

Spin coating is a very easy and relatively not expensive technique. The quality of products is usually very promising. The thickness can be easily controlled by modifications of this method.

1.3.2 Electroplating

Electroplating is a process that uses electric current to direct dissolved metal cations in solvent, so that they could form a thin coherent metal coating on an electrode. This technique is often used to modify the surface properties of target material. In this thesis, electroplating is used to deposit lead dioxide onto the surface of PEDOT: PSS film.

The process used in electroplating is called electrodeposition. It is analogous to a galvanic cell acting in reverse. The part to be plated is the cathode of the circuit.

3-electrode electroplating system is a widely used electrochemical system in many relative studies. It is composed of 3 different electrodes: working, reference and counter electrode and electrolyte. Electrolyte usually contains the reactants that the targeted reaction needs and has a good conductivity. The solvent itself need to be carefully chosen so it would not influence the target reaction.

Fig.1-9 shows the sketch of electroplating system. Each electrode has its own purpose.[38] Working electrode is the electrode where the interested reaction occurs. Thus, materials with high conductivity and high stabilities are usually utilized as working electrode. Both organic and inorganic samples can be analyzed by chemically modified electrodes.

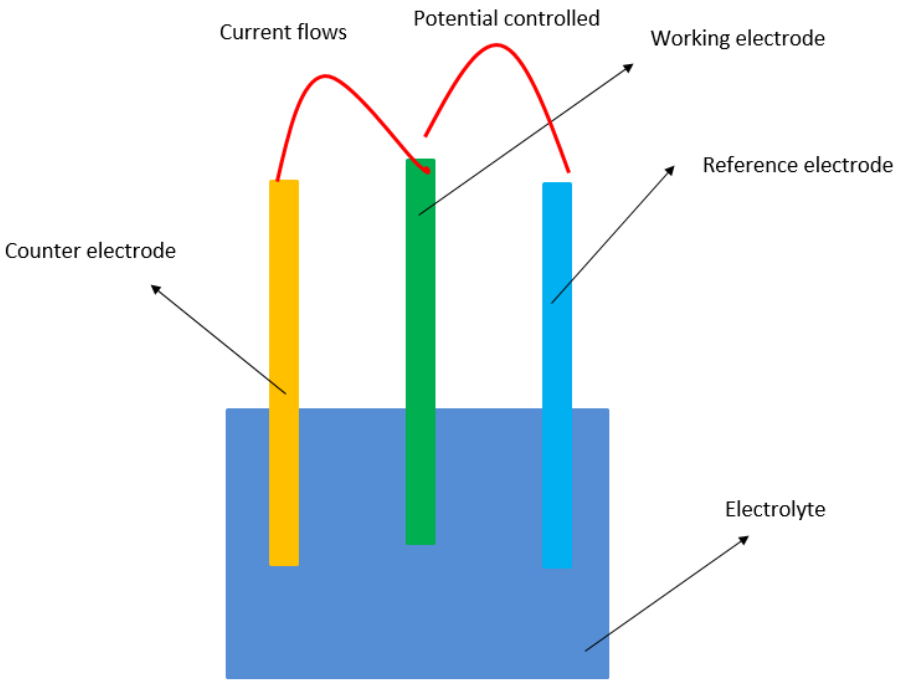

Fig.1-9 Sketch of 3-electrode electroplating system.

Reference electrode provides a stable potential during the working process of the system. The potential of working and counter electrodes may change during the reaction that happens in the system. In order to detect the precise potential of working and counter electrodes, reference electrode is needed. If the potential of counter electrode stays the same or have a rather slight change during the procedure, the reference electrode can be absent from the system.

Counter electrode is used in the system to form an electron loop with working electrode. This structure makes sure that the wanted reaction can happen at the working electrode while the mechanism of the reaction can also be studied. The material used for counter electrode should have small resistance and the size used is normally 5 times larger than the size of working electrode.

There are two electrical circuits in the 3-electrode system. Working and reference electrode form one circuit to make sure the reaction happens in suitable or proper condition. Working and counter electrode form another in order to construct a circuit to transport electrons.

The way a three electrode potentiostat works is to read the potential difference between the reference electrode and the working electrode using a very small DC current. By comparing the potential measured to the desired voltage level as input using function generator, one can adjust the voltage of the counter electrode until the difference between the desired voltage and the measured voltage is zero.

The main advantage of a three-electrode experiment over a two-electrode experiment is that the results are more stable. For two electrode system, the counter electrode is theoretically used as reference electrode. The potential of the counter electrode in a cell going through electrochemical reaction is changing all the time. The obtained results, as a consequence, are not stable.

2. Experimental

This thesis is aiming at producing the n-type and perovskite layer of organic-inorganic hybrid perovskite solar cell while understanding the characteristics. Each layer of the cell was studied to reach the optimize condition. The main procedures can be roughly divided into several steps in terms of the layers. Brief introductions about the progress will be given in this chapter and detailed information will be given in the next chapter. Fig.2-1 illustrates the target device of this thesis.

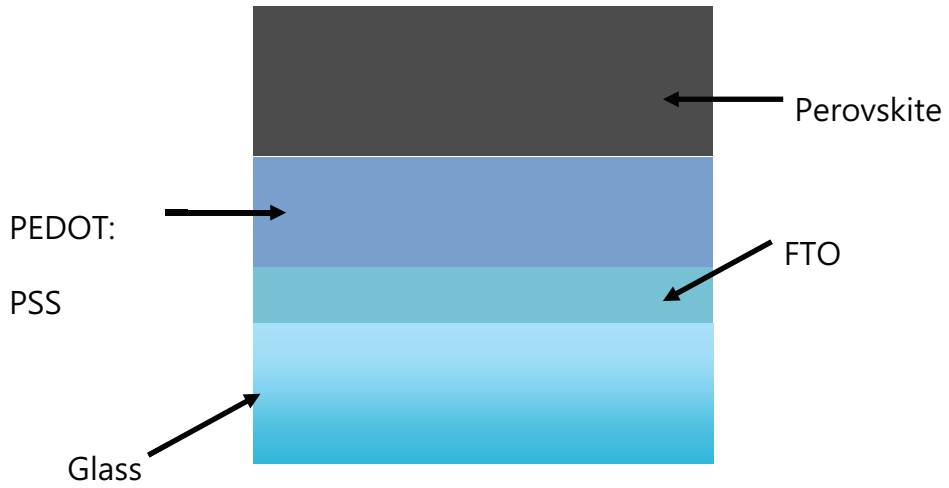

Fig. 2-1 Target device of this work.

As one can see from figure 2-1, FTO coated glass was used as substrate. It is a transparent material that light can easily go through. The first layer coated on top of the substrate is PEDOT: PSS layer, which is a conduction polymer that can also be used as a n-type semiconductor. Perovskite is built upon the PEDOT: PSS layer working as the core layer of the solar cell. Different methods were tried out during the exploring process and finally detailed producing methods which lead to stable production performance are reviewed.

2.1 Equipment and Chemicals

Raman spectroscopy is a technique often used to observe and determine vibrational modes of molecules. The technique is used to detect the inelastic scattering of photon known as Raman scattering.IR (infrared) spectroscopy is a technique used to detect the absorption of certain wavelengths of infrared light. Certain molecular can only absorb

certain wavelength of infrared light. The above-mentioned techniques are used in this work to measure the product qualitatively.

Main equipment:

Equipment	Manufacture/Model
Spin coater	Ossila
Thermostatic water bath tank	-
Potentiostat	Autolab/PGSTAT101
Raman spectroscope	Renishaw
IR spectroscope	Bruker/VERTEX70
Hot plate	-
Ultrasonic cleaner	VWR/USC-THD
Plasma cleaner	Harrick Plasma

Main chemicals:

Chemicals	Manufacture/Detail
Acetone	VWR chemicals/ Technical
Ethanol	Denaturoitu etanoli/ ETAX A7
Deionized water	-
HI	Alfa Aesar / 57% w/w aq. soln., stab with 1.5% hypophosphorous acid
PEDOT: PSS	Aldrich/ 1.3% dispersion in water
KCl	FF-Chemicals Ab
$K_3[Fe(CN)_6]$	Merck
$Pb(CH_3COO)_2$	Merck
$NaNO_3$	Merck
HNO_3	Sigma-Aldrich/ 65%
DMSO	Merck
Zonyl	Merck
Hellmanex	Sigma-Aldrich
H_2O_2	Merck

2.2 Procedures

2.2.1 PEDOT: PSS Layer

The target surface needs to be cleaned in advance to get rid of contaminations which might sabotage the performance of the whole device. FTO coated glass used is with 2 sizes (2.5cm*2.5cm and 1.0cm*1.0cm) and it is directly purchased from a factory.

First of all, FTO side of the glass needs to be detected by multimeter in order to eliminate the contact contamination as much as possible. Once the FTO side is known, carefully place the substrates on the sample holder for cleaning while remembering the facing. Fig. 2-2 shows the sketch of sample holder.

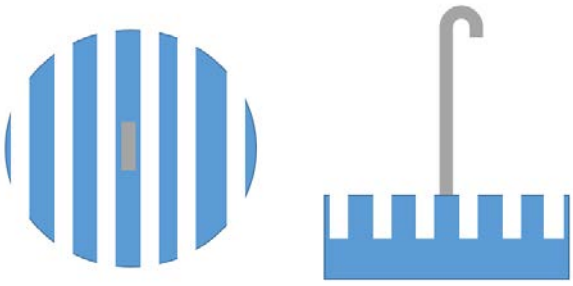

Fig. 2-2 Sketch of sample holder (top view and front view).

Three different cleaning methods for substrate were utilized to determine which one gives the best result. The comparison of the results was tested simply by using spin coater to form PEDOT: PSS thin films with same experimental conditions except for the substrate obtained by different cleaning methods.

Detailed information of 3 different cleaning methods are described below.

(1) ***Plasma cleaning***. Use the ultrasonic cleaning device to clean the FTO glass which submerged in acetone for 10 min, and do the same procedure with ethanol and deionized water respectively. After that, air flow is used the dry the substrates. Finally, use plasma cleaning device to clean the wafers under 1400mTorr O_2 atmosphere for 4 min.

(2) ***H_2O_2 cleaning***. Use the ultrasonic cleaning device to clean the FTO glass which submerged in acetone for 10 min, and do the same procedure with ethanol and deionized water respectively. Prepare a solution of deionized water: NH_3:H_2O_2. Heat

the solution up to 80℃, ultrasonic clean the wafers in it for 10min. At last, dry the wafers with air flow.

(3) ***Hellmanex Cleaning***. (Hellmanex is a kind of surfactant widely used for the cleaning of substrates). At first, make a deionized water solution with 5%(V/V) of Hellmanex. Put wafers in the solution and use ultrasonic to clean the wafers in 50℃ for 5min. Then, use boiled deionized water to remove the Hellmanex. After that, put the wafers into new deionized water. (To make sure Hellmanex was washed away as much as possible). Then put the substrates in to IPA, ultrasonic bath in around 100℃ for 5 min. Dip the cleaned substrates into freshly boiled deionized water for 2 times. Final step is to dry the wafers with air flow.

Different parameters of spin coating were tested to get a most efficient and budget-saving combination for PEDOT: PSS film forming upon the substrate. The parameters that influence the outcome of the film are as following: temperature of PEDOT: PSS solution, volume of solution used, dropping methods, spin speed, spin time, sintering time, sintering temperature.

Dropping methods for spin coating contains two ways of placing liquid on top of the target substrate, name as Dynamic method and Static method respectively. Dynamic method means placing solution on top of substrate while the substrate is spinning. On the other hand, Static method means putting solution on top of the substrate before the spin coater starts to work.

2.2.2 Perovskite Layer

Perovskite film is obtained by a combination of electroplating and chemical conversion in this thesis. The main idea is to build a perovskite layer by forming a lead dioxide layer on top of PEDOT: PSS and then chemically convert the PbO2 layer into lead iodide and finally lead iodide can be manipulated to react with MAI, perovskite film on top of PEDOT: PSS can be made.

In order to electroplate lead dioxide film onto PEDOT: PSS film, a potentiostat is used. A new electrochemical cell was built to accomplish this task. Fig.2-3 shows details of the system.

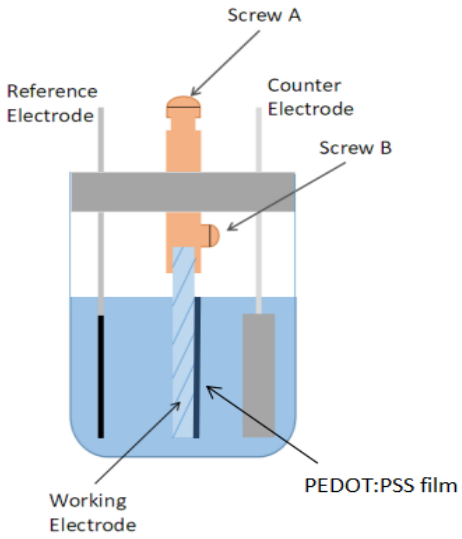

Fig.2-3 sketch of the cell used in electrodeposition of PbO_2.

The cell is sealed as the reaction is highly sensitive to air, especially oxygen. It mainly consists of 3 electrodes: reference electrode (Ag/AgCl), counter electrode (Pt) and working electrode.

Ag/AgCl is stable in high temperature and not as poisonous as an also commonly used reference electrode-calomel electrode. In water, AgCl has a low resolvability as 10^{-5} (25°C), while in saturated KCl water solution, it has a resolvability of 10 g/L. Light would accumulate the decomposition of AgCl, it is recommended to keep the electrode away from direct light.

Working electrode is PEDOT: PSS deposited FTO glass, the FTO side facing counter electrode for better quality of lead dioxide film. Every few times of deposition, the counter electrode must be cleaned by burning. To make lead dioxide film good quality, counter electrode needs to have a large surface area. Screw A enable easy contact with the potentiostat, while screw B can be adjusted to fix the working electrode. The holder for the working electrode is made of metal. During the experiment, electrolyte must not contact the metal holder, otherwise it would give unstable currents and poor film quality.

After the lead dioxide film was successfully put onto the PEDOT:PSS film, the film coated FTO glass into HI solution to convert lead dioxide to lead iodide, and then put lead iodide to MAI solution to convert it to $MAPbI_3$. These two procedures are both chemical conversions.

3. Results and Discussion

Before any experiment is carried, performance of the film needs to be defined. When the formed film is fully covered and no apparent defect can be seen virtually, the result is considered as a good one. To simplify the descriptions of experimental conditions, short forms will be applied in the text below. For instance:

Plasma clean, D(S), 1000rpm, 60s, PEDOT: PSS 45μL (50℃), 110℃ in oven for 15 min (110℃ on hot plate 15 min)

represents that the substrate is cleaned using plasma cleaning method, it is Dynamic spin coated (Static spin coated) with a spin speed of 1000rpm for 60s. 45μL of 50℃ PEDOT: PSS solution was used. After the coating, the substrate was put into an oven of 110℃ and sintered for 15min (After the coating, the substrate was put onto a hot plate of 110℃ and sintered for 15 min).

All the experiments carried in this thesis follow the rule of single variable. The conclusions mentioned in the following text are out of comparison.

In order to make the surface of substrate more hydrophilic and easier for PEDOT: PSS to be coated on, substrate cleaning methods and modifications of PEDOT: PSS were combined to find a best combo of parameters that will prohibit most ideal result.

There are some modifications can be done with the PEDOT: PSS solution. Increasing the hydrophilicity of solution itself by adding some surfactant is what this experiment used. Different volume of DMSO and Zonyl were added into the PEDOT: PSS solution as surfactants. Four kinds of various assemblies were measured.

(1)Only PEDOT: PSS.
(2)5%(V/V) of DMSO + PEDOT: PSS.
(3)10%(V/V) of DMSO + PEDOT: PSS.
(4)5%(V/V) of [5%(W/W) Zonyl + DMSO] + PEDOT: PSS.

In total, 3 kinds of mainstream substrate cleaning methods (as mentioned in chapter two) and 4 kinds of modifications of PEDOT: PSS solution were combined and tested in the same parameters of spin coating:

D, 1000rpm, 60s, PEDOT: PSS 45μL (50℃), 110℃ in oven for 15 min

Under the same conditions of spin coating, Plasma cleaned substrate coated with PEDOT: PSS solution without any surfactant, surprisingly, give out the best result.

3.1 Spin Coating of PEDOT: PSS Film

It is unknown whether the size and shape influences the result or not. FTO glass with different standards were tested. FTO glass with the size of 1.5cm*1.5cm and 2.5cm*2.5cm were spin coated using same parameters as following:

Plasma clean, D, 1000rpm, 60s, 10%(V/V) DMSO + PRDOT: PSS, 45μL(50℃), 110℃ in oven for 15min.

Four samples were made. Sample 1,2 are smaller ones and sample 3 and 4 are 2.5cm*2.5cm in size. The surface of small substrates is fully covered, while that of the large substrates are not. In the corner of the small plates, a condensation of solution can be seen.

Fig.3-1 shows the UV-vis spectra of samples. One can tell from the spectrum that all samples have quite similar absorbance although they are with different sizes. The absorbance is different even for 2 samples with same size, although the difference is small.

It is speculated that the size of wafers does not influence the results, in another word, a certain amount of area of wafer can only be coated with a certain amount of solution, and the amount of solution must be within a range with a small difference between maximum and minimum. Substrates with size of 2.5cm * 2.5cm were chosen. The following experiments are based on 2.5cm * 2.5cm FTO glass.

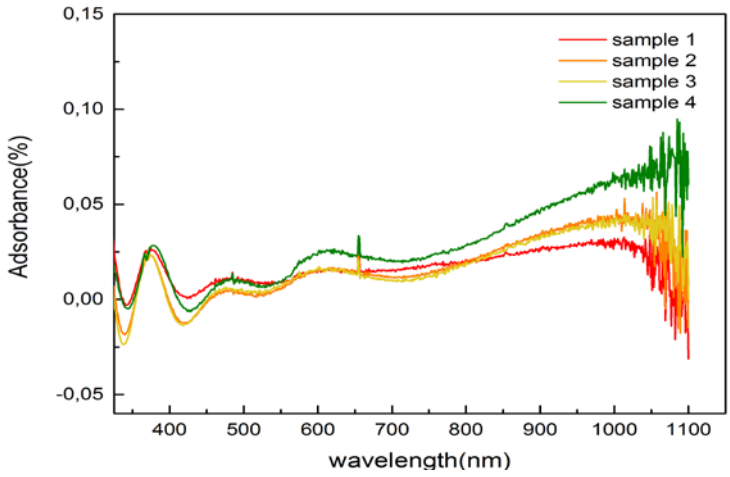

Fig.3-1 UV-vis spectra of samples with different sizes.

It is speculated that the size of wafers does not influence the results, in another word, a certain amount of area of wafer can only be coated with a certain amount of solution, and the amount of solution must be within a range with a small difference between maximum and minimum. Substrates with size of 2.5cm * 2.5cm were chosen. The following experiments are based on 2.5cm * 2.5cm FTO glass.

Different solution, volume of solution, spin methods and speed of spin were combined to find a best combination of experimental conditions.

The experimental set is named as Group A. It was tested out under these conditions:

Plasma clean, 110℃ in oven for 15min

Table. 3-1 Different experiment conditions for Group A.

Sample number	**Solution**	**Volume(μL)**	**Spin method**	**Time of spin(s)**	**Spin speed(rpm)**
1	5%DMSO+ PEDOT: PSS	300	S	30	1000
2	5%DMSO+ PEDOT: PSS	300	S	30	2000
3	PEDOT: PSS	350	S	30	2000
4	PEDOT: PSS	350	D	30	2000
5	PEDOT: PSS	350	D	30	1500
6	PEDOT: PSS	100	D	30	1500

Sample 1 was not recorded. Only sample number 4 and sample number 5 was fully covered. The UV-vis spectra of samples are showed below in Fig.3-2.

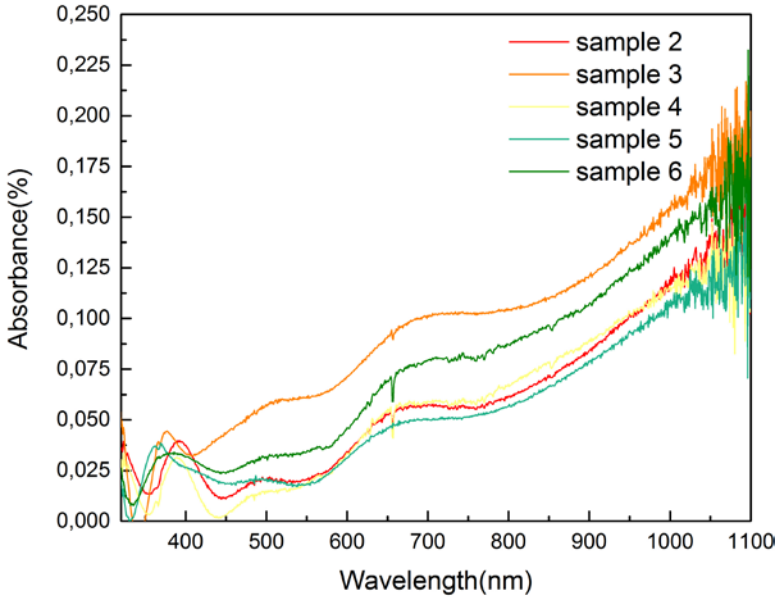

Fig.3-2 UV-vis spectrum of samples in Group C.

For FTO glass substrate, 350μL volume of PEDOT: PSS is more than surfactant for the coverage, much solution was spread out the surface when spin coating. Another experiment group is added to find the minimum volume for PEDOT: PSS that can cove the whole area of substrate.

Experiment group as Group B is carried out under conditions below:

Plasma clean, D, 1500rpm, 30s, D, 5%(V/V) of [5%(W/W) Zonyl + DMSO] + PEDOT: PSS, 110℃ in oven for 15min

Table. 3-2 Different experiment conditions for Group B.

Sample number	**Volume(μL)**
1	100
2	50
3	35
4	45
5	50
6	100

Sample 5 and 6 are made to test the repeatability. Only sample 1 and 2 are fully covered, however, for the repeat sample 5 and 6, the results are poor. This is because during the spin coating process, the solution is slowly cooled down with time. It is clear that the temperature of solution has an influence on the performance of coated films. Also, one can deduct that when decrease the volume of solution, the thickness of coated film is decreased.

When using dynamic spin coating, how to operate the pipette may also have some influences on the final results. Thus, experiment set Group E is arranged.

Plasma clean, D, 1500rpm, 30s, 5%(V/V) of [5%(W/W) Zonyl + DMSO] + PEDOT: PSS, 110℃ in oven for 15min

Table. 3-3 Different experiment conditions for Group E.

Sample number	**Volume(μL)**	**Manipulation**
1	100	Squeeze fast
2	100	Not fast, but continuously
3	100	Drop by drop
4	45	Not fast, but continuously
5	45	Drop by drop
6	45	Repeat sample 4
7	100	Repeat sample 2

The results are not good enough, partially because of the uncontrolled temperature of solution, partially because of the ways to operate dynamic spin coating. Also, from UV-vis spectra, one can realize that the thickness of the central part of sample is different from it of the edge part. Central part is thicker than edge part.

From results mentioned, 3 different cleaning methods and 4 kinds of different solutions give similar results. Therefore, plasma clean and pure PEDOT: PSS were chosen to be efficiency.

Experiment Group C is organized to study how temperature of solution influences the outcomes. The samples were spin coated under the conditions of:

Plasma clean, D, 1000rpm, 30s, PEDOT: PSS, 80μL(solution kept in oven of different temperatures for 5min), 110℃ in oven for 15min

Table. 3-4 Different experiment conditions for Group C.

Sample Number	Solution Temperature (℃)	Volume(μL)
1	30	-
2	35	-
3	40	-
4	45	-
5	50	-
6	50	90
7	50	100
8	50	100

Sample 8 is aiming to test the repeatability. None of the sample is not fully covered. The UV-vis spectra center area of Group E is showed below in Fig.3-3.

The temperature does not seem to influence the results much in this case. However, the temperature in the earlier experiments might be even lower than the lowest temperature in this experiment. The only conclusion can be obtained is that the solution with a temperature not lower than 35℃ have little influence on the results. In all the following experiments, the solution was kept warm during the coating process.

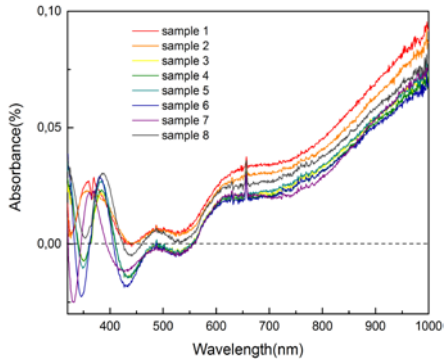

Fig.3-3 UV-vis spectrum of experiment Set E.

From this part, all the following experiments use hot plate for sintering. Two samples of PEDOT: PSS layer were made on FTO glass using same experimental conditions except

for PEDOT: PSS volume. Sample A used 200µL of PEDOT: PSS solution while sample B used 120µL of PEDOT: PSS solution. Fig.3-4 shows the microscope images of sample A and sample B.

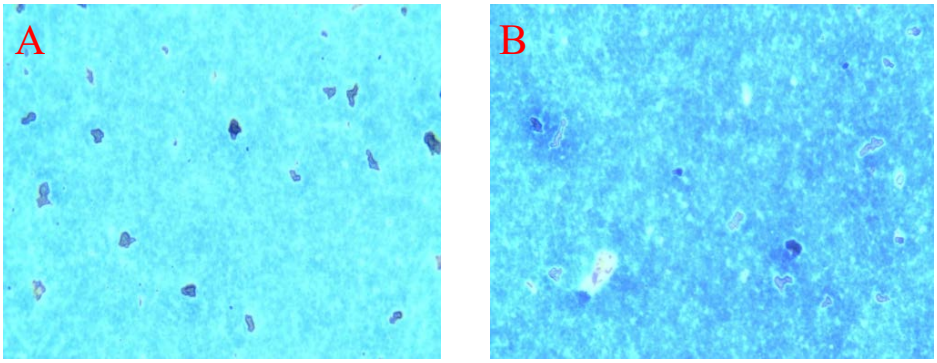

Fig.3-4 Microscope images (x50) of PEDOT: PSS layer on top of FTO. A) 200µL; B) 120 µL.

Samples produced using PEDOT: PSS solution with 2 kinds of volume do not show huge differences in appearance. Dark spots and background in sample A as well as dark spots and background in sample B were tested using Raman microscopy. They all shown peaks of PEDOT: PSS around 1440cm^{-1} [33] as shown in fig.3-5.

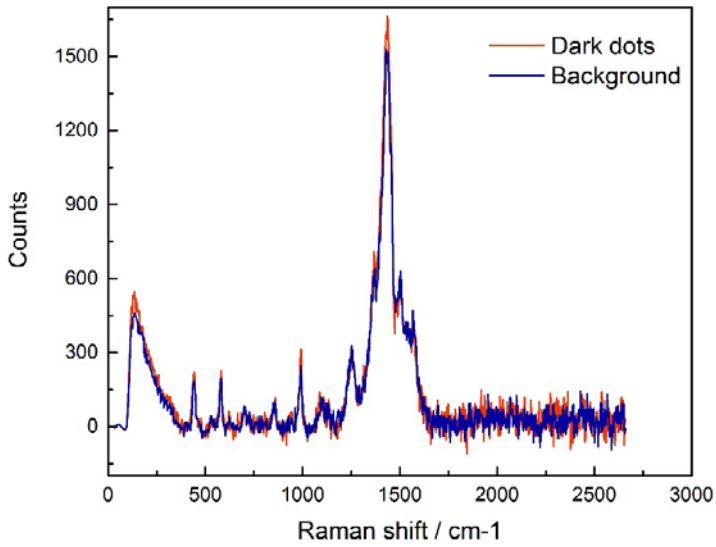

Fig.3-5 Raman spectroscopy of different morphologies in Fig.3-6.

It can be deducted that the surface can only hold certain amount of PEDOT: PSS no matter how much material used for the spin coating.

4 samples of 120µL PEDOT: PSS coated on top of FTO glass were put on top of 110℃ hot plate for sintering. The duration of the process of each sample is unequal. The

effects upon the quality of samples are analyzed below. Fig.3-6 shows microscope images of 4 samples with different sintering time.

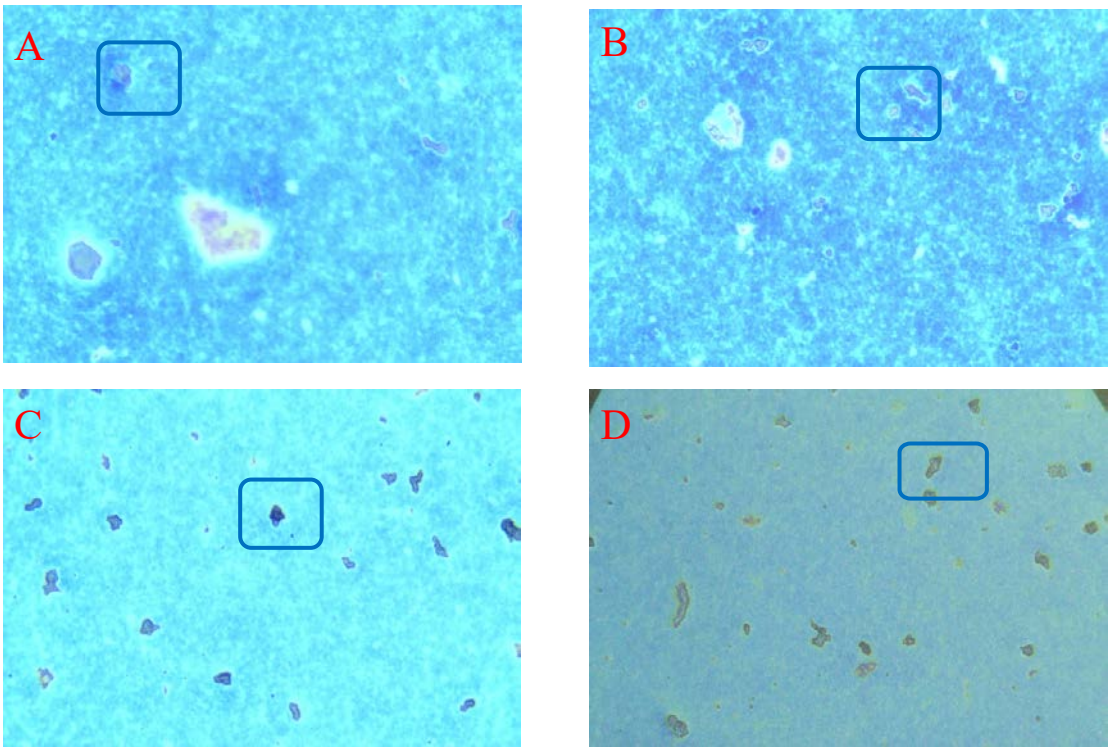

Fig.3-6 Microscope images (x50) of PEDOT: PSS layer on top of FTO. A) 2min sintering; B) 5min sintering; C) 10min sintering; D) 15 min sintering.

The spots in the blue squares are gathering of PEDOT: PSS. It is easy to obtain from the pictures that with increasing sintering time, the surface becomes more uniform. The morphology does not have an apparent change after 10 min sintering.

Fig.3-7 shows the microscope images of films coated with different PEDOT: PSS solution temperature. Samples have similar surface images. Within 10°C, the temperature does not give apparent influences on morphology of PEDOT: PSS layer. This result means that the temperature needs not to be accurately controlled in the process of spin coating.

Overall, the spin coating process has no influence on the lead dioxide or lead iodide film. As long as one can get a high-quality film of PEDOT: PSS, the operating process will not influence the final results.

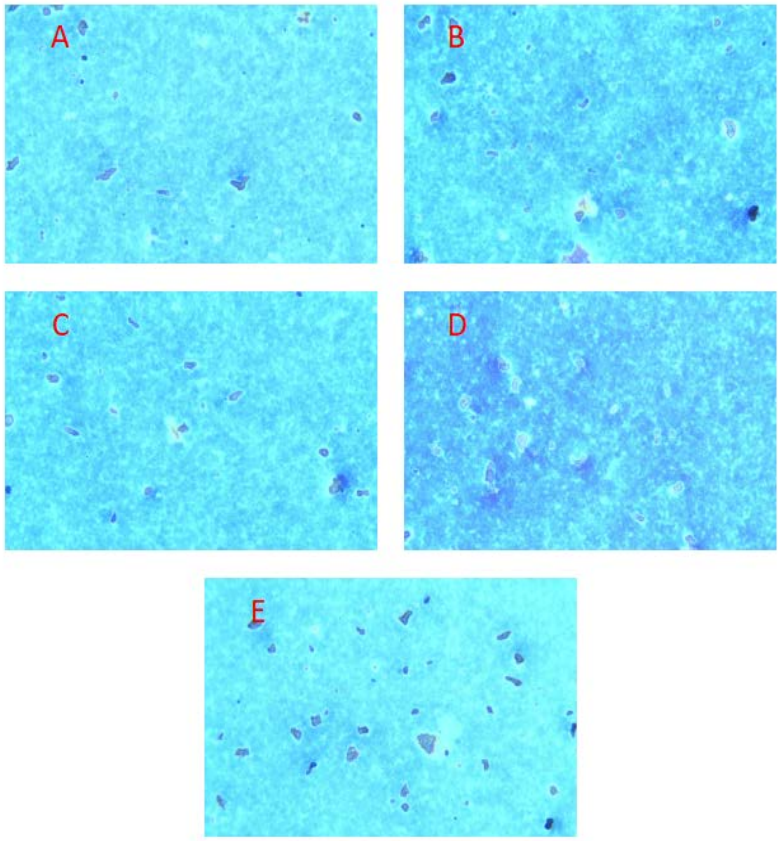

Fig.3-7 Microscope images (x50) of PEDOT: PSS layer electrodeposited on top of FTO(120μL). From A to E, the temperature of PEDOT: PSS for spin coating drops from 50°C to 40°C. Samples are made by an approximate time gap of 2min.

All the different areas in the microscope images above, shows similar signals in Raman spectroscope. This indicates that all those samples are PEDOT: PSS film.

From the experiments above, one can obtain some conclusions. Plasma cleaning gives best performance of all 3 kinds of surface clean methods. Dynamic and Static coating methods does not influence much on the result. However, under same other conditions, static dropping methods requires more solution.

The performance of different solutions has a small difference from each other, in order to save time and budget, PEDOT: PSS solution without anything is used in the later experiments. Spin speed and volume used have huge influence on the performance of films, but they depend on the combination of all the experimental parameters.

Till this step, an optimized combination of parameters for PEDOT: PSS spin coat is obtained: Plasma clean, Dynamic, 1500rpm, 30s, PEDOT: PSS, 120μL (50℃), 110℃ on hot plate for 10 min.

Fig. 3-8 shows the SEM image of the FTO glass in different magnifications.

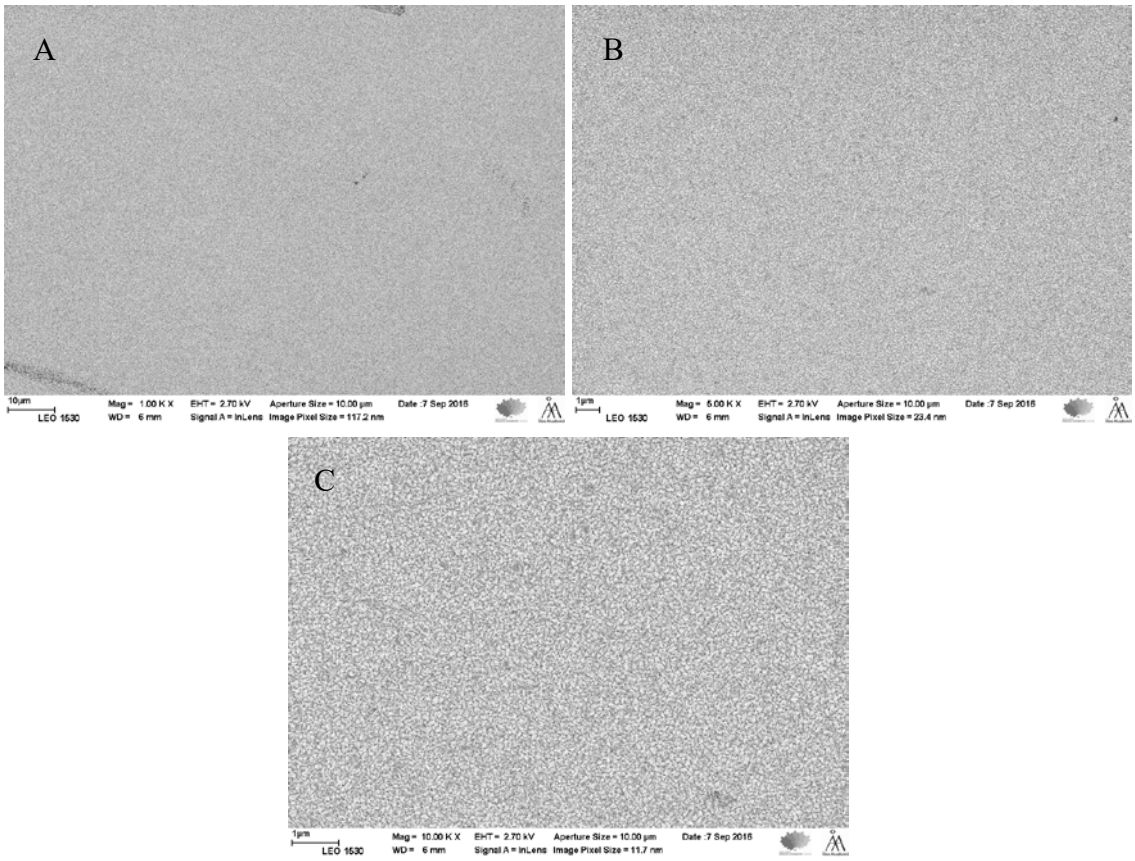

Fig. 3-8 SEM images of FTO glass. (A) 1.0 K X magnification; (B) 5.0 K X magnification; (C) 10.0 K X magnification.

From the pictures of Fig. 3-10, it is obvious that FTO layer is very smooth and uniform. In the highest magnification, small uniformed crystal grains can be observed.

The SEM images of PEDOT: PSS film obtained by the optimized combo of parameters are shown in Fig. 3-9. It shows the PEDOT: PSS SEM images in different magnifications. Comparing to FTO glass, the images of PEDOT: PSS does not show much difference. It indicates that the coated PEDOT: PSS film is too thin to be well-observed in SEM. By Raman spectroscopy, the sample show strong signals of PEDOT: PSS.

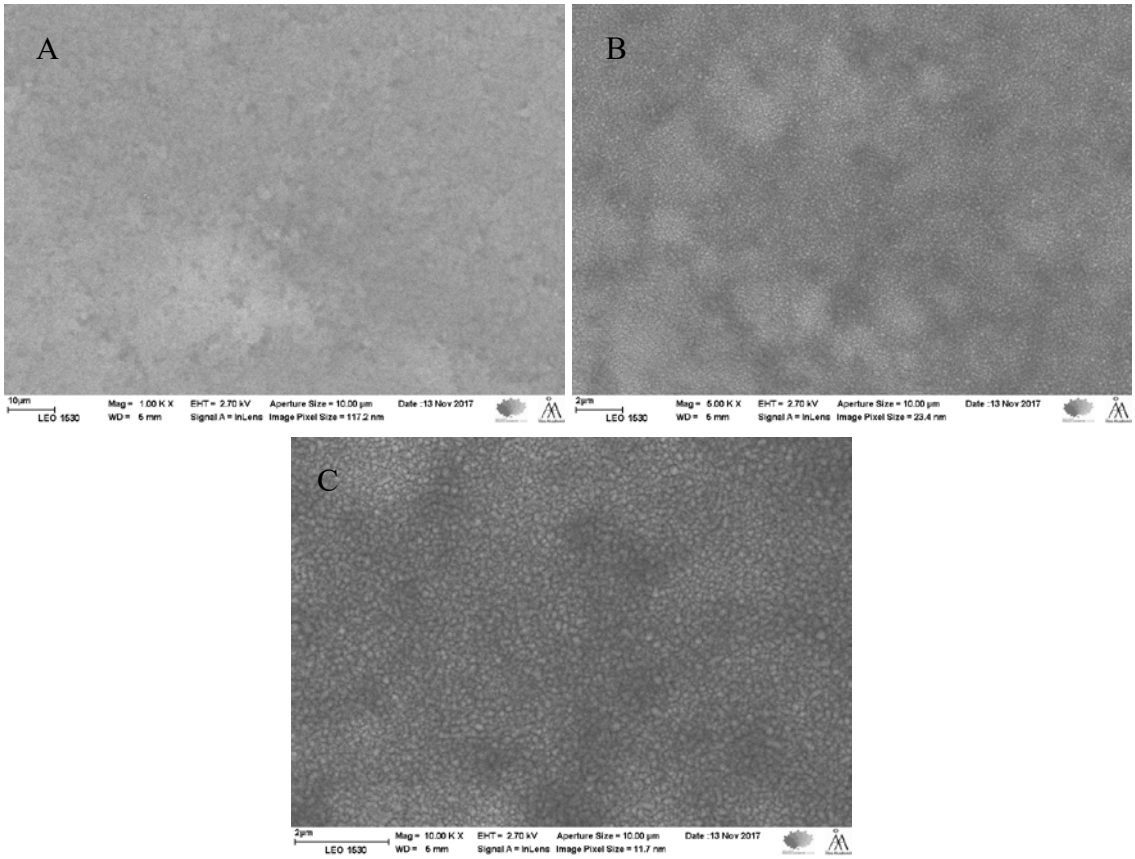

Fig. 3-9 SEM images of PEDOT: PSS film on FTO glass. (A) 1.0 K X magnification; (B) 5.0 K X magnification; (C) 10.0 K X magnification.

3.2 Electroplating of Lead Dioxide

In the process of electroplating, the counter electrode is made of Pt wire and Pt mesh. Fig. 3-10 shows the look of counter electrode.

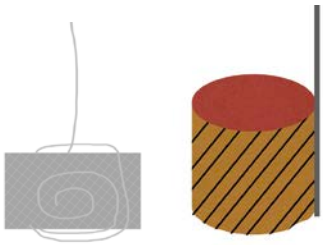

Fig.3-10 Counter Electrode made by Pt wire and mesh.

On left side of Fig.3–12 is a counter electrode consist of platinum mesh and platinum wire. On right side, is a hollow cylinder made of platinum mesh and supported by a thick platinum wire.

Theoretically, it would be good for counter electrodes to have high surface area. The platinum cylinder is more ideal than the counter electrode made of Pt mesh and wire. Both electrodes were both used in this experiment. By comparing results of two electroplated films with other conditions all same, Pt cylinder gives better performance (coverage and thickness) than the other one.

Every result in this thesis is concluded by Pt cylinder as a counter electrode.

3.2.1 Preparation

With the help of potentiostat, Ag/AgCl reference electrode can be made.

The electrolyte is saturated KCl solution. Polish Ag wire to remove the oxide on the surface, then use it as a working electrode. Pt wire is the reference and counter electrode in this experiment.

Choose chronovoltammetric mode in the potentiostat. Set the current to 0.1mA, then operate it for at least 7200s. Longer time gives more stable and durable reference electrode. The voltage- time curve of this experiment should be a line around 0.9V and 1.0V, however, some gas bubble may gather around the working electrode which would

make the curve not an even line. During the process, pay attention to the surrounding of working electrode and remove bubbles once found.

When the AgCl deposition is finished, flush the electrode with deionized water. Be aware not to touch the AgCl part whenever using the reference electrode. One reference electrode is obtained. The fresh reference electrode needs to be calibrated before put into usage. A cell needed to be built up for this procedure.

Electrolyte for calibration is consisted of the following compounds: KCl 0.373g(≈ 0.1M); K3[Fe(CN)6] 0.0825g (≈ 5mM).

Dissolve chemicals mentioned with deionized water to form 50mL solution. After the procedure, set the cell with FTO glass as working electrode, Ag/AgCl as reference electrode and Pt as counter electrode. Cyclic voltammetry potentiostatic mode in potentiostat is used in this calibration.

Detailed parameters used are shown below.

Table. 3-5 Parameters used to calibrate the reference electrode.

CV staircase	
Start potential	0V
Upper vertex potential	0.4V
Lower vertex potential	-0.4V
Stop potential	0V
Number of crossing	6
Highest current range	1mA
Lowest current range	100μA

The vertex potential range and current potential range were studied to get the best results. Before the measurement, background of the electrolyte needs to be tested to

make sure no peak of solvent shows in the vertex range used. For the electrolyte, deionized water is background. Fig.3–11 Scan of deionized water in the potential range of -0.4V to 0.4V shows that there is no peak for water in the range used.

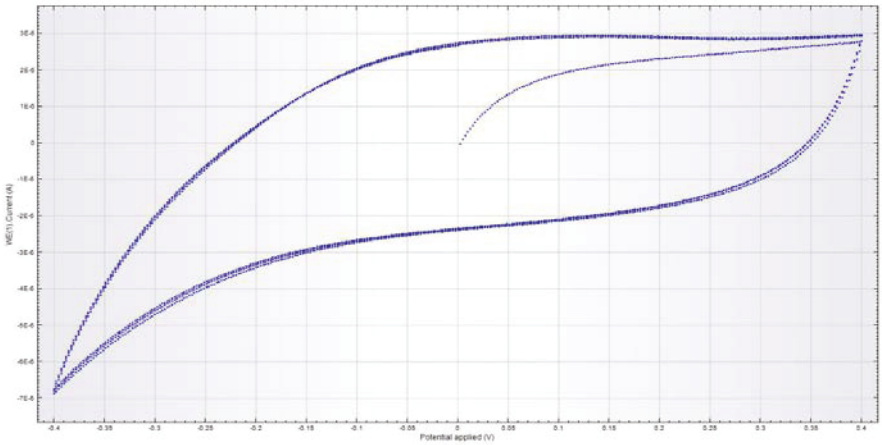

Fig.3-11 Scan of deionized water in the range of -0.4V to 0.4V.

Therefore, the electrolyte can be used for calibration now. After addition of $K_3[Fe(CN)_6]$ to the electrolyte solution, the CV shows in Fig. 3-14.

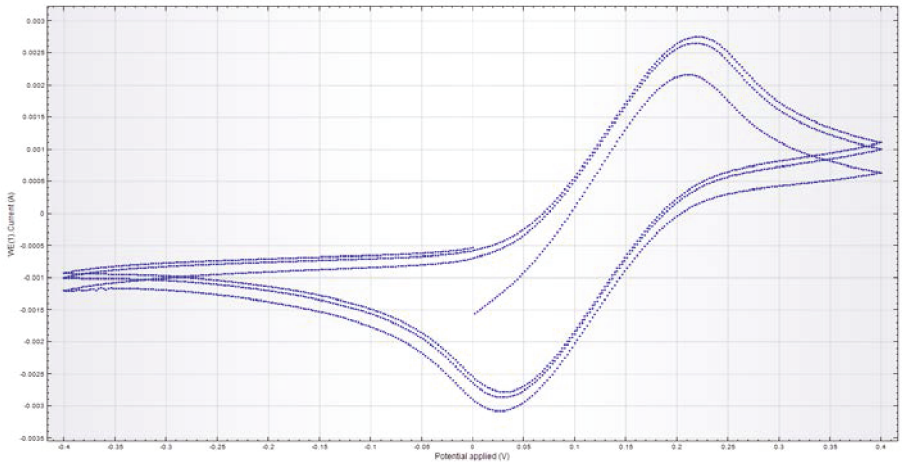

Fig.3-12 Calibration of Ag/Agcl electrode.

From Fig.3-12, one can obtain the peak positions, furthermore, the potential of the reference can be calculated. Peak position 1: 0.0366V; peak position 2: 0.2124V.

$$E = \frac{0.2124 - 0.0366}{2} V = 0.0879V$$

Thus, the reference electrode made has a potential of 0.0879V.

Theoretically, the reference electrode needed to be calibrated before and after every electroplating procedure. It is a tedious work and time-consuming procedure. In the experiments of this report, it has been tested over 100 times that the reference electrode is stable. The potential of the reference electrode remains around 0.09V before and after each experiment. Some value shifts can be seen when testing the reference value at different measurements. That is due to the electrode position change in different measures. The potential value difference is less than 0.1V which is a small value comparing to the voltage used (around 1.3V). In order to save time, calibrate once and the electrode can be used to deposit 5 times.

In the following data, calibration value for each five times will not be mentioned again due to the results are similar (around 0.09V). The reference is stable.

3.2.2 Lead Dioxide Deposition

To manipulate the parameters and make better films, one need to know the starting point of PbO_2 electrodeposition. First of all, electrolyte for deposition need to be made by dissolve 3.7935g of $Pb(CH_3COO)_2$, 1.6998g of $NaNO_3$ and 0.694mL of HNO_3 in deionized water to make a 100ml solution.

Potentiostat Mode: cyclic voltammetry potentiostatic mode.
Current range: 10mA-1mA.

The reaction scheme is shown below.

$$Pb^{2+}(l)+2OH^{-}(l)=PbO_2(s)+2H_2(g)$$

Fig.3-13 shows the starting point of the PbO_2 deposition.

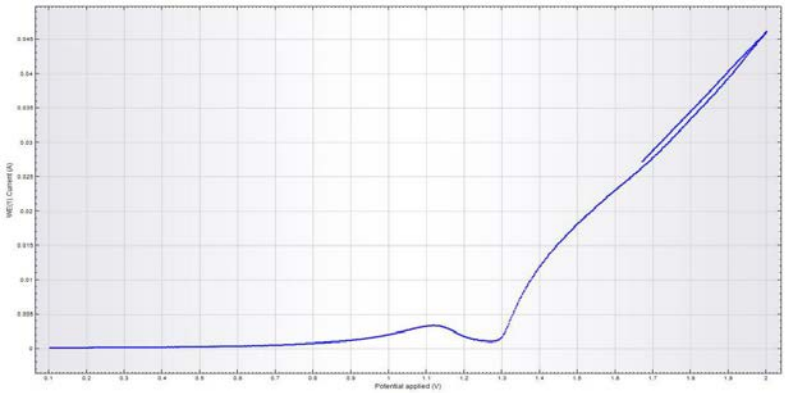

Fig.3-13 The starting point of PbO_2 deposition.

From the figure above, it is clear that PbO_2 started to deposit on the FTO surface when voltage reaches around 1.3V. Therefore, films can only be made by voltage larger than 1.3V.

Lead dioxide was deposited onto FTO/PEDOT: PSS film using different voltages and time duration. One of the attempts are shown in the Table 3-6 below.

Table. 3-6 Approaches used to produce ideal lead dioxide films.

	30s	50s	70s	90s	100s	110s	120s	150s
1.3V								
1.5V								
1.7V								
1.9V								
2.0V								
2.1V								
2.3V								

Colored area in the table is the combination of voltage and deposition time which has been tried in this experiment. Light blue represents parameter combinations lead to a fully covered surface made of reactant. Dark blue represents parameter combinations lead to not fully covered ones (Some part peels off). Yellow represent the combination shows the best product quality.

For both horizontal and vertical directions, trials stopped because the film already started to peel off from the FTO glass. Uniformed and thick films are wanted in this experiment. No hole formation is the baseline of the production procedure. Yellow squire in Table.3-8 is the best result yet.

Fix the time as 30s, the thickness increases with voltage. When reaching 2.1V, some part of lead dioxide started to peel off from the substrate. It is owing to the formation of gas bubbles around the working electrode.

Fix the voltage at 2.0V, increasing the time makes the film thicker. However, the quality is not stable. Most of the time, the film is homogeneous, but there are occasions when some holes showed on the film. The same outcome happens when using 1.5V, 1.7V, 1.9V.

Fix the voltage at 1.3V, film thickness increases with time. Lower voltage and longer time allow the film to be deposited evenly. The best result so far is made from 1.3V, 90s. There are some procedures which gives same or better results. They are, however, not used because of poor stability and repeatability.

The solution for deposition needs to be paid attention to. It must be kept away from air, otherwise some contamination might be found in samples. Theoretically, the solution can be used for many times because the concentration of Pb^{2+} is much more than needed. However, the working electrode used is 2.5cm*2.5cm FTO glass, which have a rather large area. In this case, solution needs to be replaced after few depositions. It is hard to calculate or monitor the concentration. Over 50 samples prove that the quality of lead dioxide film will not change in a large range if electrolyte is renewed every 8 times of deposition.

For the information about sintering time of PEDOT: PSS film and lead dioxide morphology on top of them, the following experiment was carried out.

The most important things considering electroplating are voltage and time. They are similar to the relationship of spin speed and volume in spin coating technique. Since the best result can be obtained by 1.3V and 90s as in Table. 3-8, detained relationships between different parameters were studied.

Under the voltage of 1.3V, lead dioxide was depositing on top of PEDOT: PSS layer for 30s. Those PEDOT: PSS layers of samples were sintered on hot plate for 2 min, 5min and 10 mins respectively.

The following figure shows microscope images of lead dioxide samples.

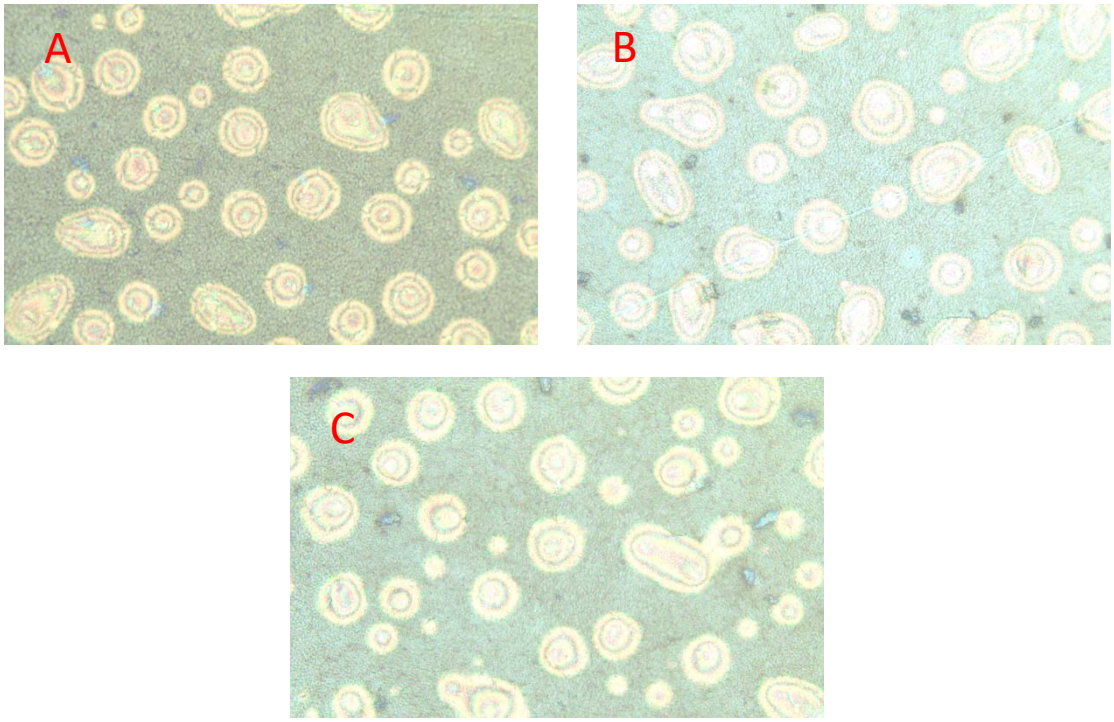

Fig.3-14 Microscope images (x50) of PbO_2 layer electrodeposited on top of PEDOT: PSS (1.3V, 90s). A) 2min sintering; B) 5min sintering; C) 10min sintering.

Fig.3-14 shows images of 3 different lead dioxide layers on FTO/PEDOT: PSS wafers for which different sintering time has been used. From the images, one can easily tell that no apparent differences upon morphology can be seen from them. It can be concluded that sintering time does not influence on the deposition of the PbO_2 layer on PEDOT: PSS. All the different morphologies in the sample were tested with Raman spectroscopy and showed same signals as lead dioxide.

Together with Fig.3-8, it is logical to deduct that sintering time can make influence on the PEDOT: PSS layer. However, it cannot influence the formation of lead dioxide layer, which means the quality of lead dioxide layer has nothing to do with sintering time of PEDOT: PSS.

The performance of samples with different electroplating time was studied as experiments below.

Sample A is deposited with 2.0V, sample B has been deposited under 1.3V.

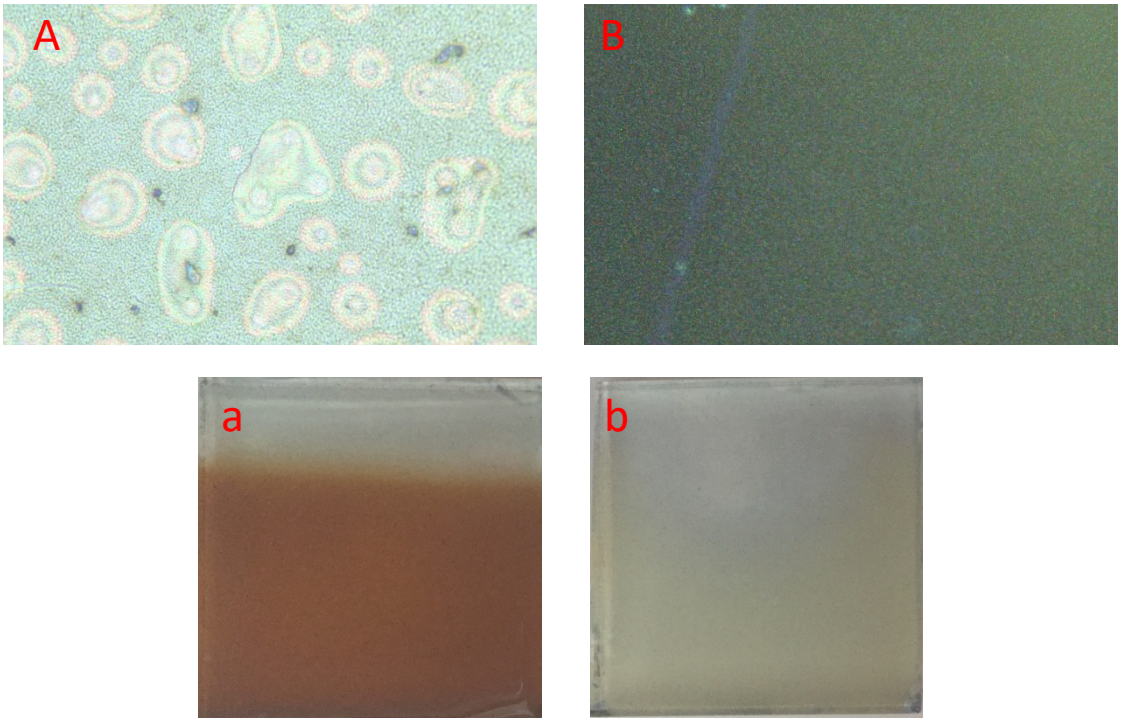

Fig.3-15 Microscope images (x50) of PbO_2 layer on top of PEDOT: PSS and sample(A and B) pictures. A) 2.0V, 30s; B) 1.3V; 30s; a) picture of sample A; b) picture of sample B.

As shown in Fig. 3-15, for sample A, obvious brown color can be seen from surface. The microscope image is similar to what have been observed with samples made with same condition. On the other hand, sample B does not show any direct information from the microscope image, the color of sample from picture is very dilute and faint. This comparison is just for the integrity of the whole experiment. Since the voltage is been decided to be 1.3V through the results of massive experiments, no other voltages shall be mentioned.

The connection between electroplating time and the performance of samples are discussed below.

As shown in Fig.3-16, samples A-G are deposited with different time under 1.3V. Barely something can be seen on the image of sample A. Very low amount of material was deposited on the surface. When using the same potential, 1.3V and prolong the time for deposition, a more condense film can be obtained.

Furthermore, samples with deposition time in the range of 90s-110s show the best results. Deposition time above 110s lead to small holes formed on the surface. 150s

deposition also gives a condense layer, but there are many holes formed, even the lead dioxide layer started to peel off.

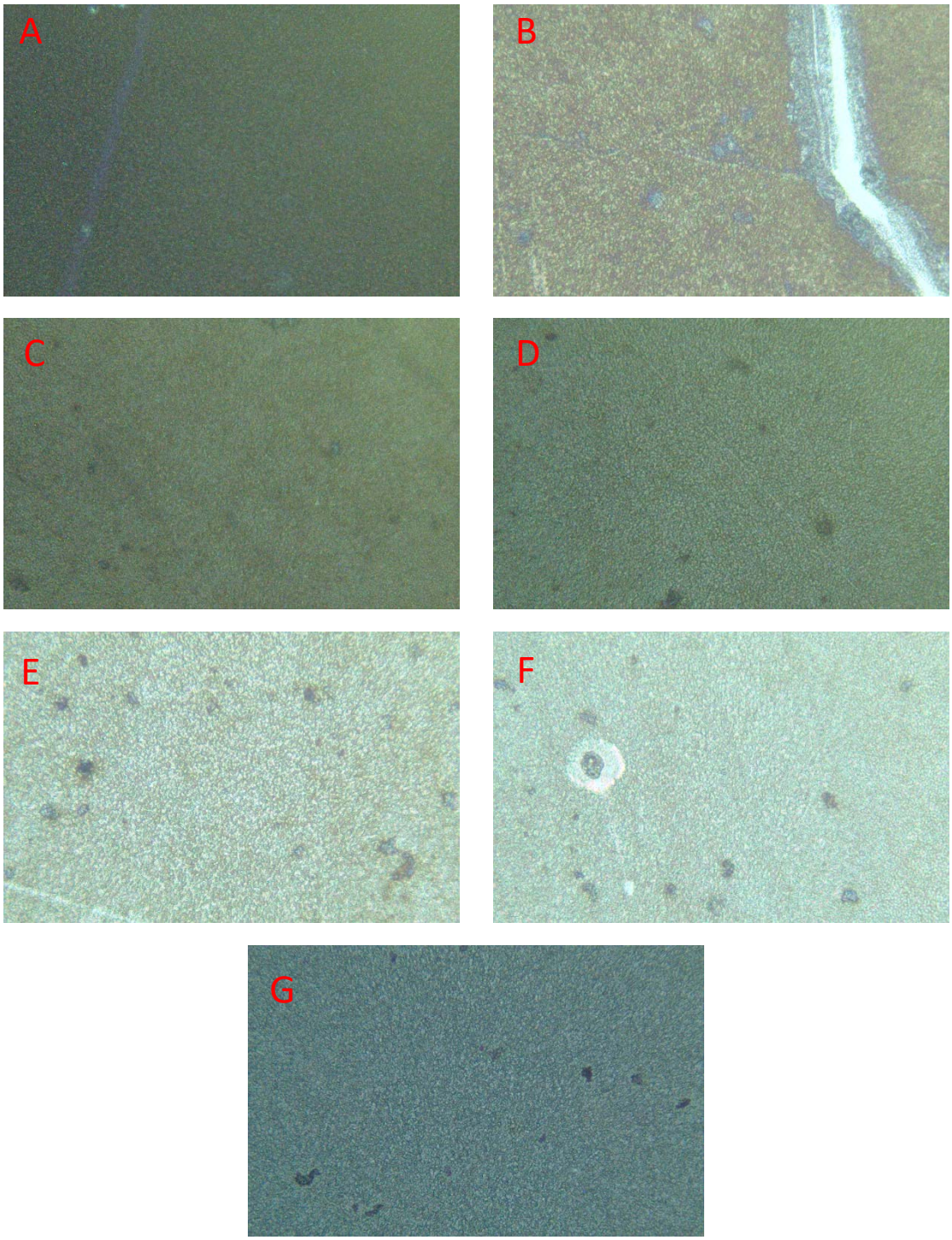

Fig.3-16 Microscope images (x50) of PbO_2 layer on top of PEDOT: PSS (120μL) of samples with different reaction time. A) 30s; B) 90s; C) 100s; D) 110s; E) 120s; F) 150s; G) 180s.

After repeatability test, lead dioxide films made through electroplating 90s under 1.3V are best in quality and repeatability among others. SEM images of lead dioxide made by electroplating 90s under 1.3V are shown below in Fig.3-17.

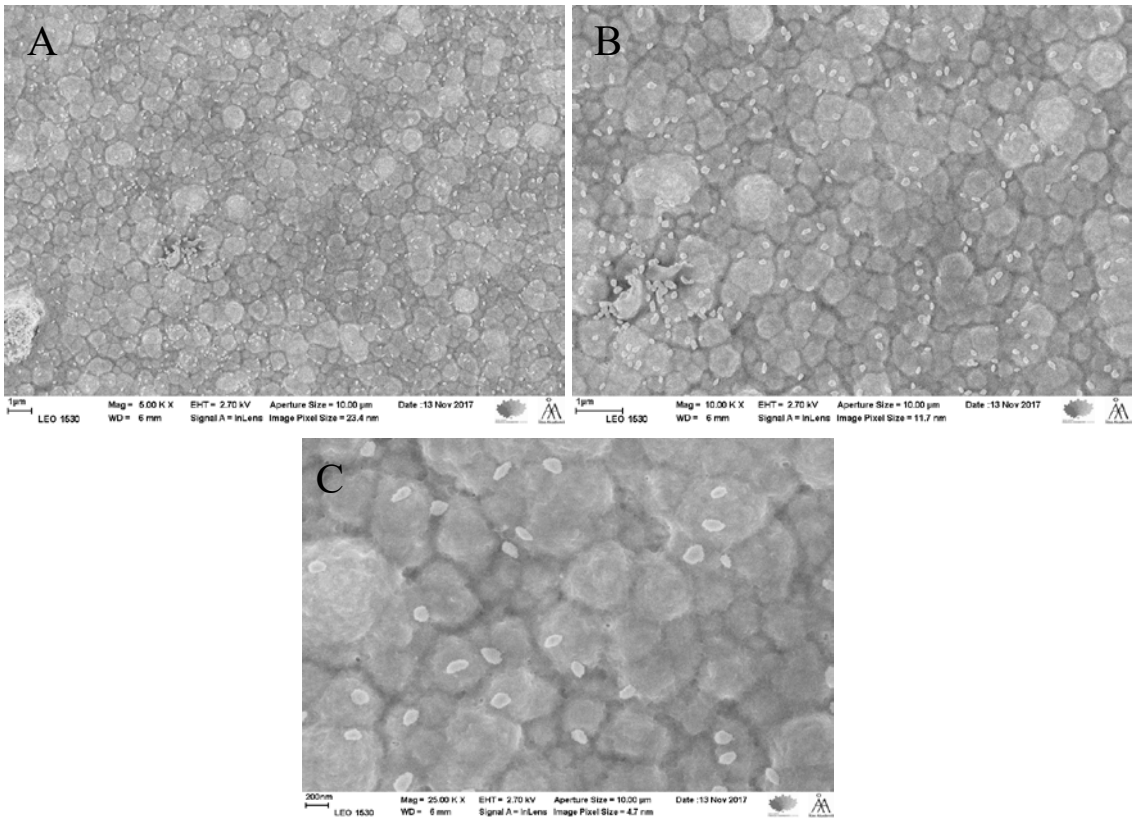

Fig.3-17 SEM images of lead dioxide film on PEDOT: PSS. (A) 5.0 K X magnification; (B) 10.0 K X magnification; (C) 25.0 K X magnification.

From the SEM, lead dioxide crystals can be clearly observed. That indicates the layer of PEDOT: PSS is covered by the crystals. White dots in pictures are less stereo than other parts, they might be some less conducting dirt particles.

In the experiments, it was also been found that the lead dioxide film is highly sensitive. Even a slight contact may leave a severe scratch. After deposition, the working electrode needs to be flushed with deionized water for cleaning. Before the conversion into PbI_2, the samples need to be carefully stored. Three different methods of storage were utilized in this part: put samples in open environment; stored in Ethanol; stored in deionized water. Ethanol and deionized water were chosen because none of them can dissolve lead dioxide.

Samples put in open surrounding shows the worst appearance. Many lines and scratches can be found. Samples stored in Ethanol and deionized water shows similar results, barely any damage can be found. Ethanol was finally determined to be the storage solution at last. It is highly volatile, so it can save much time when dry lead dioxide samples are needed.

3.3 Lead Iodide Conversion

Many approaches can be used to convert lead dioxide to lead iodide. Basically, every approach follows the fundamental chemical reaction between lead dioxide and hydrogen iodide (HI). HI was dissolved in Ethanol (0.0125M) if nothing particular was mentioned about in the following text. The reaction can be deducted as:

$$PbO_2\,(S) + 4HI(L) \rightarrow PbI_2(S) + 2H_2O(L) + I_2(S)$$

Dipping method is the easiest operating among all methods used. The overall idea is to submerge the samples into HI solution. The experiment cannot be easily controlled because the high acidity of HI.

Too concentrated solution can convert the film in a very short time and cannot be precisely controlled. On the other hand, if the concentration is much too low, the conversion can be a long progress. At one point, the film would be partly peeled off from the substrate while other parts remaining unconverted.

The crucial part of this method is adjusting the concentration and time of conversion. Only if one appropriate combination was found can the film be made even and homogeneous. With many trials, the results were still not good enough. Thus, other parameters ware introduced to the system to manipulate the film quality--temperature and solvent.

Table 3-9 shows all the combinations of time and concentration tried to manipulate the results, the temperature of the sample and HI solution is room temperature, the solvent used is Ethanol. The yellow square in Table. 3-9 indicates the best approach so far.

Light blue represents parameter combinations lead to a fully covered surface made of reactant. Dark blue represents parameter combinations lead to not fully covered ones (some part peels off). Yellow represent the combination shows the best product quality.

For the direction of time increase, trials stopped when samples began to be incomplete. As for the concentration, too dilute solution would take too much time and did not give any better results. So, it stopped when the concentration reached 1/15.

Under the best combination for concentration and time, the lead iodide film made is still not good enough. Besides, the repeatability is not stable. Thus, the temperature of template and solution was manipulated. The solvent for HI is also adjusted to make a better-quality film.

Table. 3-7 Different attempts to produce ideal lead iodide film.

	1	1/2	1/3	1/4	1/5	1/10	1/15
3min							
5min							
10 min							
15min							
20min							
30min							

1 represent the concentration of 0.125M.

Fig. 3-18 shows the comparison of two samples after further reaction with HI. Sample A was treated with a deposition time of 90s and for sample B, 110s was used respectively.

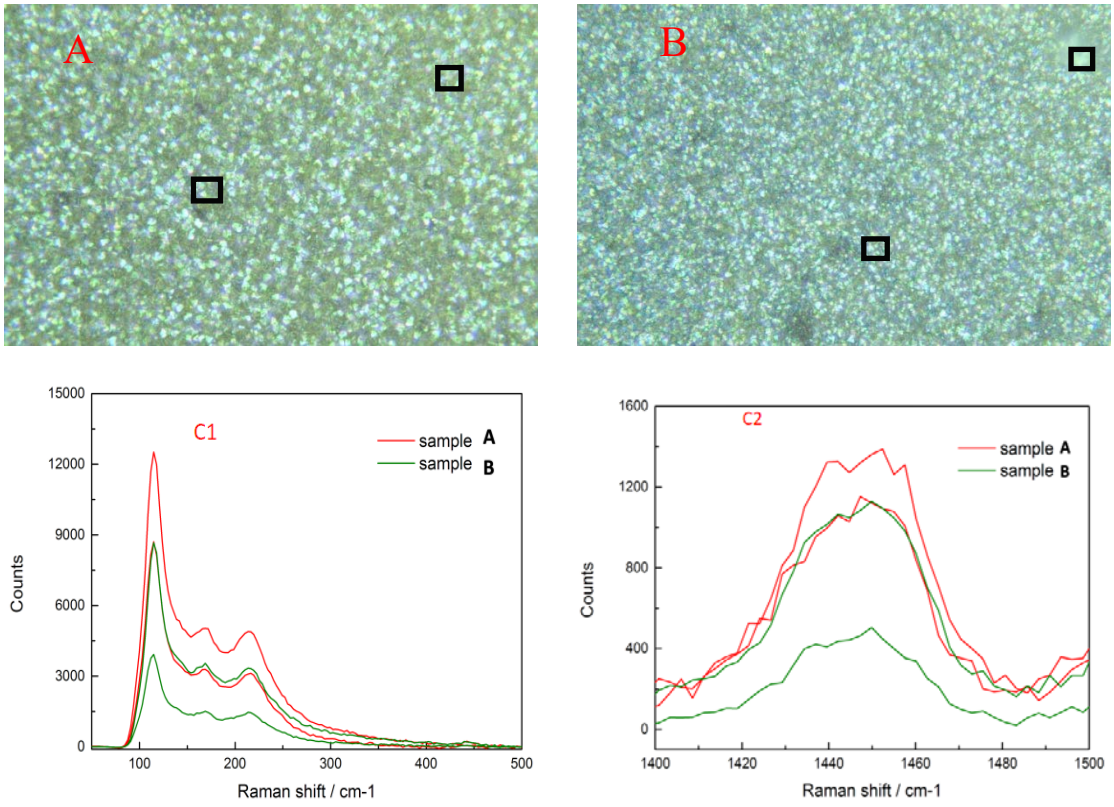

Fig. 3-18 Microscope images (x50) of PbI_2 layer on top of PEDOT: PSS and Raman spectra. A) Microscope image sample A; B) Microscope image of sample B; C1) and C2) Raman spectra for two different ranges (0-500cm^{-1} and 1400-1500cm^{-1}).

Sample A and sample B indicates similar results. There are 2 kinds of morphologies in the microscope images as showed by rectangular frames, the dark spots and the light spots. Thus, the Raman images shows two curves for each sample. Raman peak for PEDOT: PSS is around 1440 cm^{-1}, and that for lead iodide is round 100 cm^{-1}. From the images we can see that sample A and B both have strong peaks for PEDOT: PSS as well as PbI_2. However, further experiments were carried and samplers with 90s performed a better stability than 110s and 100s. Therefore, 90s is the best option so far.

Different from PEDOT: PSS layer, the quality of lead dioxide film can be told directly from the appearance of it. Therefore, the influence of electroplating upon the performance of lead dioxide is actually controlled by the quality of film formed.

Sample A and B are converted in the same concentration (0.0125M) of HI for different duration, A was submerged for 10 min, B was submerged for 15min.

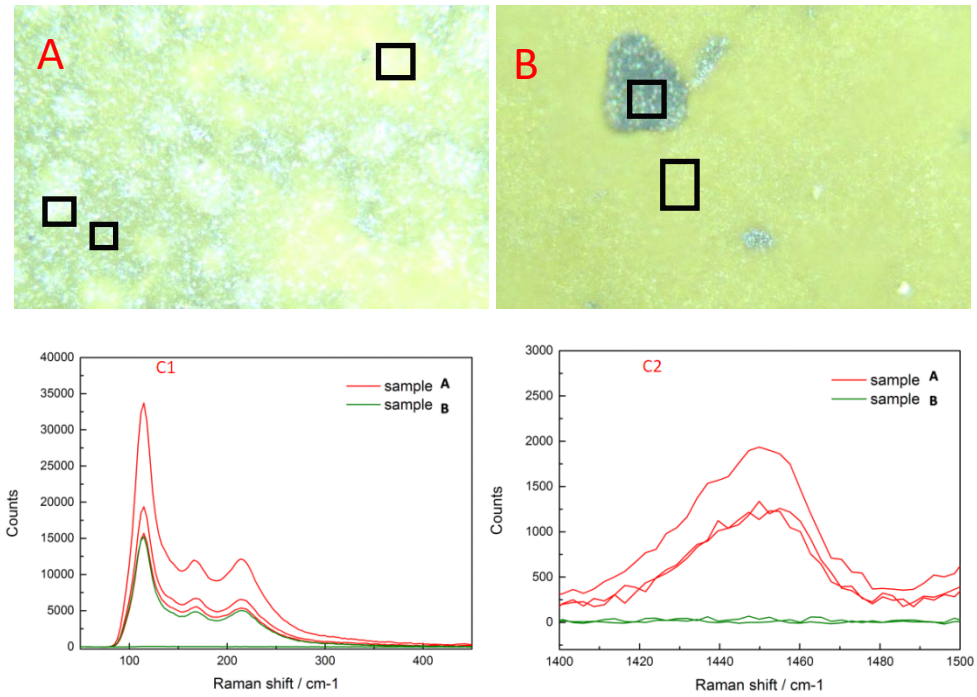

Fig. 3-19 Microscope images (x50) of PbI_2 layer on top of PEDOT: PSS and and Raman spectroscopy image. A) Microscope image sample A; B) Microscope image of sample B; C1) and C2) Raman images in different ranges.

Fig. 3-19 shows the images and Raman curves of those samples. 3 kinds of areas showed for sample A, 2 kinds areas showed for sample B as showed in the images. The light area in sample B is shows no signal while yellow area shows strong Raman signal of PbI_2. It can be ducted that: for sample B, light area is bare FTO glass while yellow area is PbI_2. Longer time performance a better surface which is more homogeneous. The signal of PbI_2 will decrease compare to shorter time conversion. During the conversion, some material have already dissolved in the solution. Ethanol was used as solvent and the temperature of solution/ substrate was controlled.

Put the substrate on 60°C hot plate for 3min, then put the warmed substrate into room temperature solution (HI 0.0125M) for 7min. High quality lead iodide film was successfully made. Lead dioxide was converted completely even when looking at the plate from the backside and no hole or peeled off area was found. Warm HI solution on 60°C hot plate for 3min, then put substrate into warmed solution for 4min. High quality film was made. Visually looks better than last one. 60°C was chosen because the boiling point of ethanol is around 70°C. In 60°C, the reaction of conversion happens faster. The quality of film also increased.

Signals of PbI_2 can be seen using Raman spectroscopy. In Raman spectroscopy, the signals from lead iodide can be seen in the range less than 100cm^{-1}, which is beyond the range of the Raman system owned by the research lab. Hence, IR spectroscopy could be an effective tool to prove the existence of lead iodide.

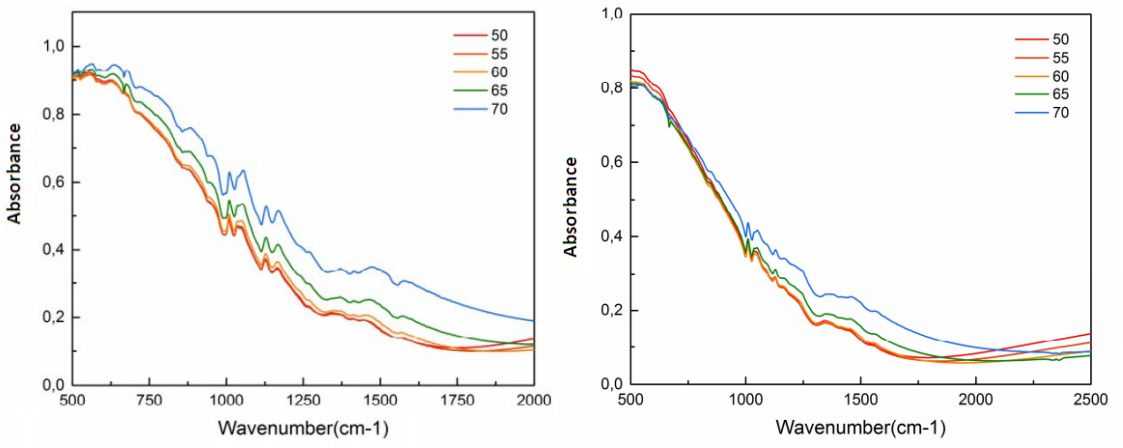

Fig. 3-20 IR curve of PbO_2 with different angles and backgrounds (PEDOT: PSS and FTO glass).

Fig. 3-20 shows IR curve of PbO_2/PEDOT: PSS and PbO_2/ FTO glass with different angles. The first spectrum uses PEDOT: PSS as background while the second uses FTO glasses. For the IR spectroscopy test, amount of scan is 64 and the resolution is 4cm^{-1}.

It can be seen from the curves that spectra gathered at 70° shows the highest absorbance of all spectra gathered. As for the background, PEDOT: PSS shows more clear results than FTO glass. Thus, 70° and PEDOT: PSS background is most ideal for the IR experiments of PbO_2.

The amount of scan is 62 and the resolution is 4cm^{-1}. The IR peak of PEDOT: PSS is around 1094 cm^{-1}. The signal is not strong enough to be sure that around 500 cm^{-1} exists signals for lead dioxide.

When changing the solvent into water, “golden rain” phenomena happens as show in Fig.3-21. Lead iodide prepared from cold solutions of Pb^{2+} and I^- salts usually consists of many small hexagonal platelets, giving the yellow precipitate a silky appearance. Larger crystals can be obtained by exploiting the fact that solubility of lead iodide in water increases dramatically with temperature. The compound is colorless when dissolved in hot water, but crystallizes on cooling as thin but visibly larger bright yellow flakes, that

settle slowly through the liquid -- a visual effect often described as "golden rain". [34] Larger crystals can be obtained by autoclaving the PbI_2 with water under pressure at 200 °C. [35]

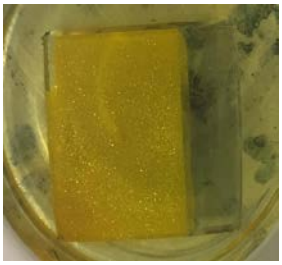

Fig. 3-21 Large crystal pieces of lead iodide owing to recrystalization, which also describes as "Golden Rain".

No matter the HI solution is heated or not, still large crystals may form in a rapid speed. Everything peels off from FTO surface within 10s. As mention in introduction, golden rain phenomena happen during recrystallization. However, no reasonable explanation can explain why this happens.

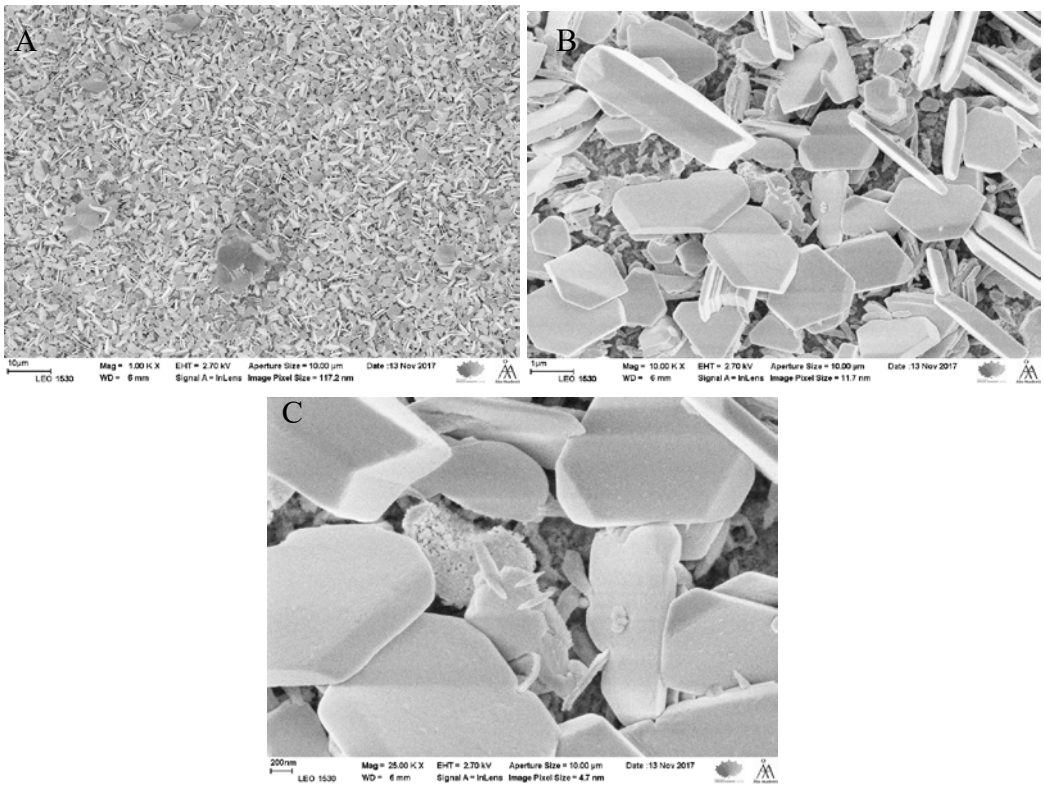

Fig.3-22 SEM images of lead iodide film on PEDOT: PSS. (A) 1.0 K X magnification; (B) 10.0 K X magnification; (C) 25.0 K X magnification.

Fig.3-22 shows the SEM images of lead iodide film on top of PEDOT: PSS. Large crystals of lead iodide can be seen in the pictures.

3.4 Perovskite Conversion

Perovskite is made by lead iodide and MAI in this thesis. The substrate covered by lead iodide in submerged in a solution of MAI isopropanol. The concentration of the solution is 10mg/mL. Converting the lead iodide for 2 hours and a good film of black perovskite is gained.

Fig.3-23 and Fig.3-24 shows SEM images of perovskite.Fig.3-25 shows the large crystal flake of perovskite. Fig.3-26 shows the small particle areas of perovskite.

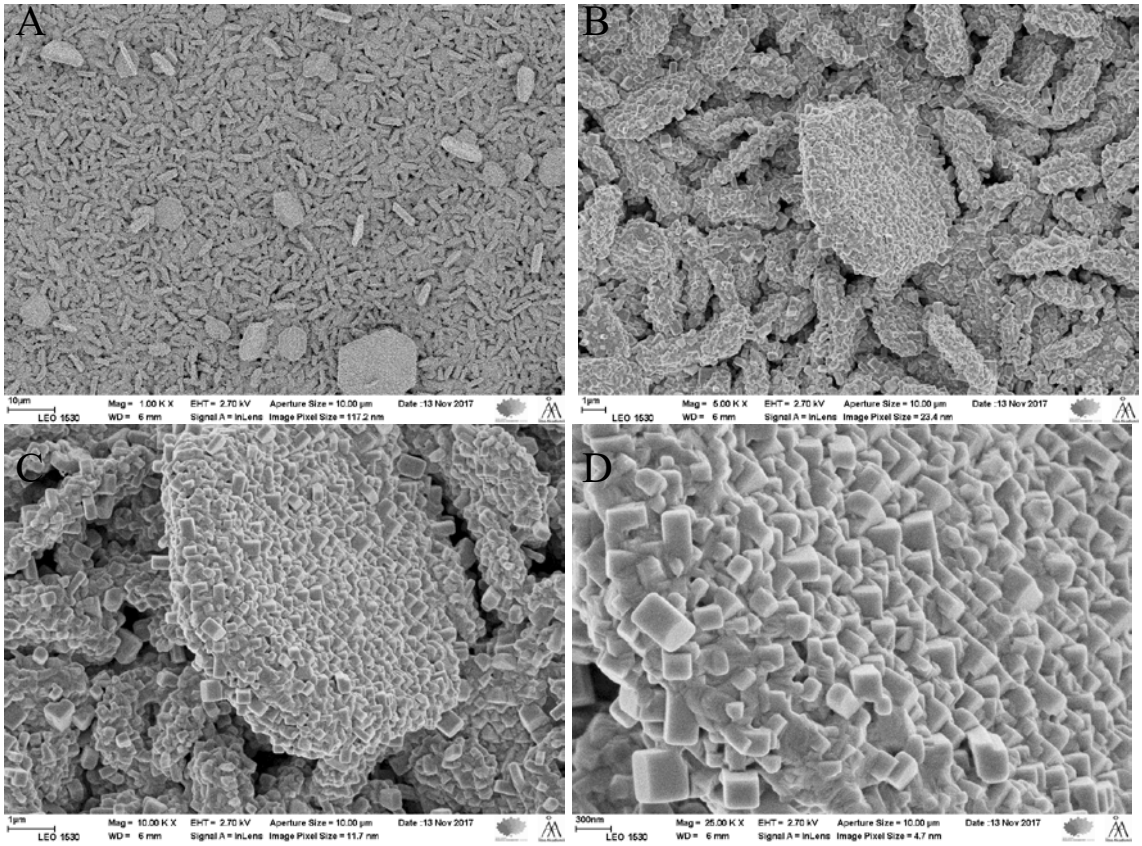

Fig.3-23 SEM images of crystal flakes of perovskite. (A) 1.0 K X magnification; (B) 10.0 K X magnification; (C) 25.0 K X magnification.

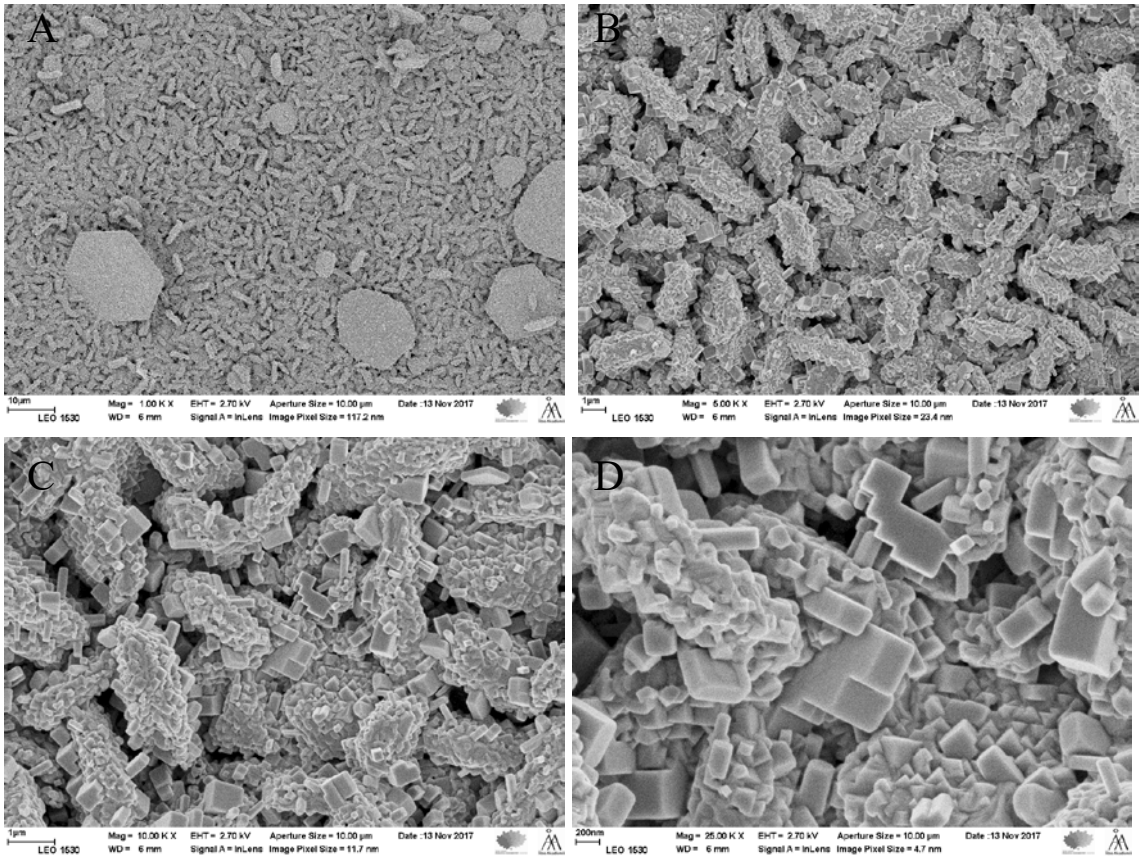

Fig.3-24 SEM images of perovskite. (A) 1.0 K X magnification; (B) 10.0 K X magnification; (C) 25.0 K X magnification.

In both flake and small crystal areas, small cubic structure of perovskite can be observed, the micro morphology in each area is similar to each other. However, when comparing to the SEM pictures of lead dioxide, apparently the crystal flakes shrink into much small sizes. This is owing to the high surface energy of lead dioxide crystal flakes and over-saturation of chemicals. When reaction happens, perovskite crystals forms with a high nucleation rate leading a small crystal size.

The degeneration phenomenon of MAPI mentioned in introduction 1.2.2 can only be observed when it is exposed long enough to moisture. Divertingly, the degradation is not exactly the same when exposing the crystal to a relatively high humidity environment or to water directly. The black color of MAPI would turn to light yellow, which is the color of lead iodide, almost immediately when contacting water. In this process, MAPI is degraded to PbI_2 and methylammonium iodide (MAI) whom are the pristine reactants of preparing MAPI.

It is mentioned that the quality of PEDOT: PSS film does not influence the quality of lead dioxide film on it. We can explain this phenomenon from the prospective of nucleation.

Classic nucleation theory (CNT) is a theoretic model to understand nucleation from a prospective of thermodynamics. This model presents the condensation of supersaturated vapors to the liquid phase and can also be applied to crystallization from solutions and melts. It can be used only under the assumption that: the reaction is in equilibrium; the nuclei is sphere; the cluster grows by one particle at one time; cluster and bulk material shares the same prosperities and interfacial energy is independent of size. The change in Gibbs free energy of the system (ΔG) during nucleation is the sum of decrease in volume energy (ΔG_V) and the increase in the interfacial energy (ΔG_S). ΔG_V is generated from chemical potential change while ΔG_S is generated from the formation of surfaces. Nucleation depends on the Gibbs free energy change in system. ΔG of nucleation of nucleus with a radius of r can be present as:

$$\Delta G = -\frac{4\pi r^3}{3v_1}\Delta\mu + 4\pi r^2 \cdot \sigma$$

$\Delta\mu$ is the chemical potential difference between solid and liquid, σ is the interfacial energy between the liquid and solid per unit area, and v_1 is the molecular volume of the liquid. By deformation of the equation, one can get the relationship between size and ΔG is shown in Fig 3-25.

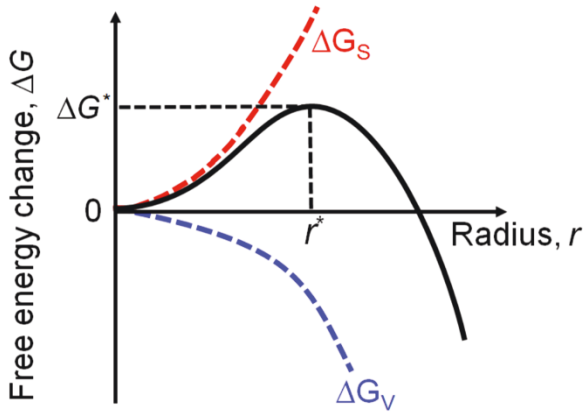

Fig 3-25 Relationship between radius and ΔG according to CNT.

ΔG^* is the critical Gibbs free energy change and r^* is the critical size. When the size of cluster is smaller than r^*, the cluster will dissolve and vice versa the cluster will spontaneously grow larger when size is larger than r^*.

For electrodeposition system, an electric field is applied across the working electrode in such a way as to give electrons to the ions in solution so that they form uncharged elements or compounds which prefer to adhere to the surface of the working electrode rather than remain dissolved in solution.[40] For lead dioxide deposition, electrons generated will react with electrolyte and produce lead dioxide particles. This particles adhere to the PEDOT:PSS surface and forms lead dioxide layer. The adherence process can be seen as the heterogeneous nucleation of lead dioxide. For stable system, the interfacial free energy does not change. The quality does not have an influence on the crystallization thus does not influence the quality of lead dioxide film.

For the conversion of lead iodide and perovskite, both of the experiments are chemical conversions. From the SEM photos and reaction equations, one can deduct that the conversion is actually exchange of ions. The morphology of former reactant layer, concentration of solution, surface energy of crystals and other influences can all contribute to the final morphology of the crystal layer.

From the experiments above, stable results can be obtained. In order to increase the property of the perovskite film, some enhancements may be taken into consideration. The concentration of MAI solution could be decreased to compensate the fast nucleation of perovskite crystal, thus to produce larger crystals.

4. Conclusion

Repeatable high-quality perovskite film can be made by the optimized combination of parameters: plasma clean the substrate, then use Dynamic dipping method coating 50℃ 120μL of PEDOT: PSS by a spin coater at 1500rpm for 30s, finally, put the coated substrates on a hot plate of 110℃ for 10 min. Repeatable high-quality lead dioxide film can be made by electroplating in 1.3V for 90s. Repeatable high-quality lead iodide film can be made by dipping into 60°C 0.0125M HI ethanol solution for 4min. Repeatable perovskite film can be made using chemical conversion by dipping the lead iodide coated substrates into MAI isopropanol solution for 2min. With the process so far, PEDOT: PSS layer/ lead dioxide and PEDOT: PSS/ lead iodide is strongly combined together.

References

[1] Q.F. Dong, Y.J. Fang, Y.C. Shao, P. Mulligan, J. Qiu, L. Cao, J.S. Huang, Electron-hole diffusion lengths 4 175 mm in solution-grown $CH_3NH_3PbI_3$ single crys- tals, Science 347 (2015) 967–970.

[2] S. Bai, Z. Wu, X. Wu, Y. Jin, N. Zhao, Z. Chen, Q. Mei, X. Wang, Z. Ye, T. Song, R. Liu, S.-t Lee, B. Sun, High-performance planar heterojunction perovskite solar cells: preserving long charge carrier diffusion lengths and interfacial engineering, Nano Res. 7 (2014) 1749–1758.

[3] S.D. Stranks, G.E. Eperon, G. Grancini, C. Menelaou, M.J.P. Alcocer, T. Leijtens, L. M. Herz, A. Petrozza, H.J. Snaith, Electron-hole diffusion lengths exceeding 1 mm in an organometal trihalide perovskite absorber, Science 342 (2013) 341–344.

[4] Z. Guo, J.S. Manser, Y. Wan, P.V. Kamat, L.B. Huang, Spatial and temporal imaging of long-range charge transport in perovskite thin films by ultrafast microscopy, Nat. Commun. 6 (2015) 7471.

[5] A. Kojima, K. Teshima, Y. Shirai, T. Miyasaka, Organometal halide perovskites as visible-light sensitizers for photovoltaic cells, J. Am. Chem. Soc. 131 (2009) 6050–6051.

[6] L. Etgar, P. Gao, Z. Xue, Q. Peng, A.K. Chandiran, B. Liu, M.K. Nazeeruddin, M. Graetzel, Mesoscopic $CH_3NH_3PbI_3/TiO_2$ heterojunction solar cells, J. Am. Chem. Soc. 134 (2012) 17396–17399.

[7] M.M. Lee, J. Teuscher, T. Miyasaka, T.N. Murakami, H.J. Snaith, Efficient hybrid solar cells based on meso-superstructured organometal halide perovskites, Science 338 (2012) 643–647.

[8] A. Mei, X. Li, L. Liu, Z. Ku, T. Liu, Y. Rong, M. Xu, M. Hu, J. Chen, Y. Yang, M. Gratzel, H. Han, A hole-conductor-free, fully printable mesoscopic per- ovskite solar cell with high stability, Science 345 (2014) 295–298.

[9] P. Docampo, J.M. Ball, M. Darwich, G.E. Eperon, H.J. Snaith, Efficient organo-metal trihalide perovskite planar-heterojunction solar cells on flexible poly- mer substrates, Nat. Commun. 4 (2013) 2761.

[10] http://www.science-kick.com/solar-cell-type/device-architectures

[11] G. Adam, M. Kaltenbrunner, E.D. Głowacki, D.H. Apaydin, M.S. White et al., Solution processed perovskite solar cells using highly conductive PEDOT:PSS interfacial layer. Sol. Energy Mater. Sol. Cells 157, 318–325 (2016). doi:10.1016/j.solmat. 2016.05.011

[12] Golschmidt, V. M. (1926). "Die Gesetze der Krystallochemie". Die Naturwissenschaften. 21 (21): 477–485. Bibcode:1926NW.....14..477G. doi:10.1007/BF01507527.
[13] Megaw, Helen (1945). "Crystal Structure of Barium Titanate". Nature. 155 (3938): 484–485. Bibcode:1945Natur.155..484.. doi:10.1038/155484b0.
[14] Baikie, T., Fang, Y., Kadro, J. M., Schreyer, M., Wei, F., Mhaisalkar, S. G., … White, T. J. (2013). Synthesis and crystal chemistry of the hybrid perovskite (CH3NH3)PbI3 for solid-state sensitised solar cell applications. Journal of Materials Chemistry A, 1(18), 5628.
[15] Baikie, T., Fang, Y., Kadro, J. M., Schreyer, M., Wei, F., Mhaisalkar, S. G., … White, T. J. (2013). Synthesis and crystal chemistry of the hybrid perovskite (CH3NH3)PbI3 for solid-state sensitised solar cell applications. Journal of Materials Chemistry A, 1(18), 5628.
[16] Baikie, T., Fang, Y., Kadro, J. M., Schreyer, M., Wei, F., Mhaisalkar, S. G., … White, T. J. (2013). Synthesis and crystal chemistry of the hybrid perovskite (CH3NH3)PbI3 for solid-state sensitised solar cell applications. Journal of Materials Chemistry A, 1(18), 5628.
[17] Baikie, T., Fang, Y., Kadro, J. M., Schreyer, M., Wei, F., Mhaisalkar, S. G., … White, T. J. (2013). Synthesis and crystal chemistry of the hybrid perovskite (CH3NH3)PbI3 for solid-state sensitised solar cell applications. Journal of Materials Chemistry A, 1(18), 5628.
[18] Leguy, A. M. A.; Hu, Y.; Campoy-Quiles, M.; Alonso, M. I.; Weber, O. J.; Azarhoosh, P.; van Schilfgaarde, M.; Weller, M. T.; Bein, T.; Nelson, J.; Docampo, P.; Barnes, P. R. F. Reversible Hydration of CH3NH3PbI3 in Films, Single Crystals, and Solar Cells. Chem. Mater. 2015, 27, 3397−3407.
[19] Z. Zhu, V. G. Hadjiev, Y. Rong, R. Guo, B. Cao, Z. Tang, F. Qin, Y. Li, Y. Wang and F. Hao, Chem. Mater., 2016, 28, 7385–7393.
[20] J. A. Christians, P. A. Miranda Herrera and P. V. Kamat, J. Am. Chem. Soc., 2015, 137, 1530–1538.
[21] J. Yang, B. D. Siempelkamp, D. Liu and T. L. Kelly, ACS Nano, 2015, 9, 1955–1963.
[22] Manser, J. S., Saidaminov, M. I., Christians, J. A., Bakr, O. M., & Kamat, P. V. (2016). Making and Breaking of Lead Halide Perovskites. Accounts of Chemical Research, 49(2), 330–338.
[23] Manser, J. S., Saidaminov, M. I., Christians, J. A., Bakr, O. M., & Kamat, P. V. (2016). Making and Breaking of Lead Halide Perovskites. Accounts of Chemical Research, 49(2), 330–338.
[24] Hao, F.; Stoumpos, C. C.; Liu, Z.; Chang, R. P. H.; Kanatzidis, M.

G. Controllable Perovskite Crystallization at a Gas−Solid Interface for Hole Conductor-Free Solar Cells with Steady Power Conversion Efficiency over 10%. J. Am. Chem. Soc. 2014, 136, 16411−16419.
[25] Frost, J. M., Butler, K. T., Brivio, F., Hendon, C. H., van Schilfgaarde, M., & Walsh, A. (2014). Atomistic origins of high-performanc1. Frost, J. M. et al. Atomistic origins of high-performance in hybrid halide perovskite solar cells. Nano Lett. 14, 2584–90 (2014).e in hybrid halide perovskite solar cells. Nano Letters, 14(5), 2584–90.
[26] Manser, J. S.; Reid, B.; Kamat, P. V. Evolution of Organic− Inorganic Lead Halide Perovskite from Solid-State Iodoplumbate Complexes. J. Phys. Chem. C 2015, 119, 17065−17073.
[27] Yan, K.; Long, M.; Zhang, T.; Wei, Z.; Chen, H.; Yang, S.; Xu, J.Hybrid Halide Perovskite Solar Cell Precursors: The Colloidal Chemistry and Coordination Engineering behind Device Processing for High Efficiency. J. Am. Chem. Soc. 2015, 137, 4460−4468.
[28] Guo, Y.; Shoyama, K.; Sato, W.; Matsuo, Y.; Inoue, K.; Harano, K.;Liu, C.; Tanaka, H.; Nakamura, E. Chemical Pathways Connecting Lead(II) Iodide and Perovskite via Polymeric Plumbate(II) Fiber. J. Am. Chem. Soc. 2015, 137, 15907−15914.
[29] Williams, S. T.; Zuo, F.; Chueh, C.-C.; Liao, C.-Y.; Liang, P.-W.;Jen, A. K.-Y. Role of Chloride in the Morphological Evolution of Organo-Lead Halide Perovskite Thin Films. ACS Nano 2014, 8, 10640− 10654.
[30] C. Bi, Y. Shao, Y. Yuan, Z. Xiao, C. Wang, Y. Gao and J. Huang, J. Mater. Chem. A, 2014, 2, 18508–18514.
[31] C. Bi, Q. Wang, Y. Shao, Y. Yuan, Z. Xiao and J. Huang, Nat. Commun., 2015, 6, 7747.
[32] Y. Deng, E. Peng, Y. Shao, Z. Xiao, Q. Dong and J. Huang, Energy Environ. Sci., 2015, 8, 1544–1550.
[33] Satoshi Sakamoto, Masanori Okumura, Zinggang Zhao, Yukio Furukawa, Chemical Physics Letters, Volume 412, Issues 4–6, 2005, 395-398,
[34] Declan Fleming (2015): Golden rain. Education in Chemistry video. Accessed on 2016- 08-25.
[35] Xinghua Zhu, Peihua Wangyang, Hui Sun, Dingyu Yang, Xiuying Gao, Haibo Tian (2016) Facile growth and characterization of freestanding single crystal PbI2 film. Materials Letters, volume 180, pages 59–62. doi:10.1016/j.matlet.2016.05.101
[36] You, J., Yang, Y. (Michael), Hong, Z., Song, T.-B., Meng, L., Liu, Y., … Yang, Y. (2014). Moisture assisted perovskite film growth for high performance solar cells. Applied Physics Letters, 105(18), 183902.

[37] Ag, N. (2014). Materials Chemistry A, 1750–1756.
[38] Dufour & 2006 IX-1.
[39] https://en.wikipedia.org/wiki/PEDOT:PSS
[40] https://wwwru.uni.lu/recherche/fstc/physics_and_materials_science_research_unit/research areas/photovoltaics/research/electrodeposition

Support information

Electroplating lead dioxide onto Microporous Glass

Due to the high price of FTO glass and the economic-friendly principle of this experiment, normal microporous glass (2.5cm*2.5cm) were introduced to mimic the FTO glass. It is much cheaper to use microporous glass exploring a technique as spin coating who has many aspects involved that may influence the result. By finding a good combination of parameters of spin coating on microporous glass, the similar results are expected to coincide with FTO glass.

For the study of how different spin methods (Dynamic and Static) influence the outcome of coating, microporous glass was cleaned by Plasma cleaning method and coated under the following conditions:

D(S), 1000rpm, 1000rpm, 60s, PEDOT: PSS, 45μL (50℃), 110℃ in oven for 15min

Two samples were made using Dynamic coating method and Static coating method respectively. Fig. S1 is the UV-vis spectrum of those samples.

One can get a conclusion easily from Fig. S1, that there is not much differences between the UV-vis spectrum of 2 methods. Conclusion can be made that the ways of how to drop the solution does not influence the results for normal microporous glass.

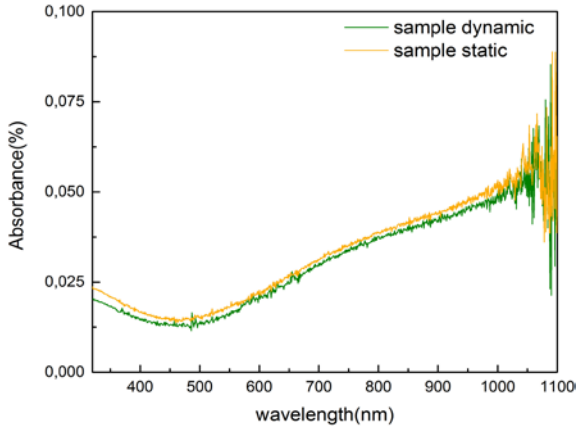

Fig.S1 UV-vis spectrum of samples using different spin coating methods.

Centrifugal force is the main mechanism of spin coating technique. Thus, it is obvious to relate the speed of rotation and the volume used to the final performance of product. With fixed conditions, relationship among products quality, speed of spin and volume used were discussed.

One Experiment group (Group A) of samples were made under the conditions:

Plasma clean, D, PEDOT: PSS, 110℃ in oven for 20 min

Table. S1 Different experimental conditions for Group A.

Sample Number	Conditions
1	A1 B1
2	A1 B2
3	A1 B3
4	A2 B1
5	A2 B2
6	A2 B3
7	A3 B1
8	A3 B2
9	A3 B3

* A1: 1000rpm; A2: 1500rpm; A3: 2000rpm

*B1: 35μL; B2: 45μL; B3: 55μL

Table. S1 describes the difference in parameters among samples. Visually, all samples are well-covered with a nice film of PEDOT: PSS. The UV-vis of each sample is shown below.

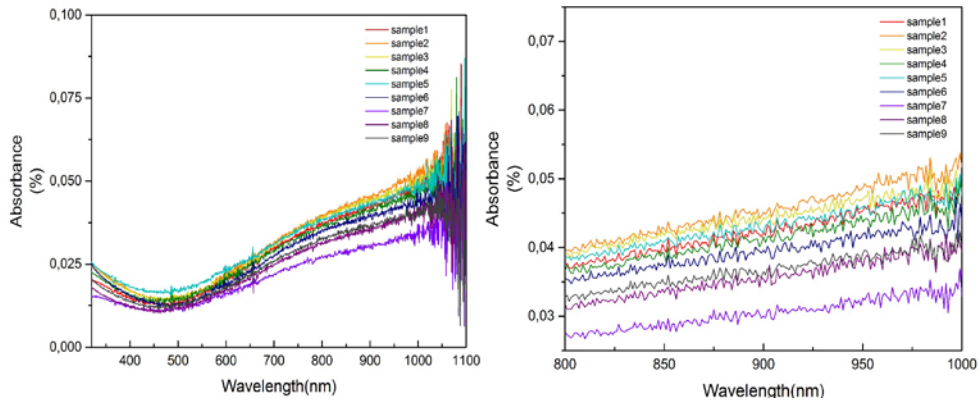

Fig. S2 UV-vis spectrum of samples in Set A with different experimental conditions. Lest side is in range

of 325nm-1100nm; right side illustrates the spectrum in range of 800nm-1000nm.

From Fig. S2 above, one can tell that the differences are quite small. It is considered that higher signals of absorption indicate thicker PEDOT: PSS formed, which is defined to be a more successful result. Hence, the best one among group A is 1000rpm, 35μL of PEDOT: PSS solution.

In order to study the influence of time in oven, time for spin coating, volume and whether dynamic method and static method influences the performance of sample when other parameters changes, the following experiments, named as Group B, was organized.

Theoretically, there are many conditions cannot be controlled in dynamic spin coating, like the drop speed, the distance from the surface to the tip of pipette and the position of deposition on the surface. Static showed similar results from dynamic, on the other hand, it is easier to control the conditions of static spin coating. Thus, static method is chosen as the basic one. Samples are coated under the following conditions.

Plasma clean, 1000rpm, PEDOT: PSS, oven 110℃

Visually, all samples are all fully covered by PEDOT: PSS. AFM, UV-vis spectrums of each sample and comparison of them were obtained.

In Group B, the time in oven does not influence the outcome at range of 15min and 20 min. Overall, the longer time for spinning, the thinner film will be got. Dynamic and static does not influence the outcomes much. Higher volume gives stronger signal of absorption.

Table. S2 Different experiment conditions for Group B.

Sample number	Volume(μL)	Spin method	Time of spin(s)	Sintering
1	55	S	60	Oven 20min
2	55	S	60	Oven 10min
3	110	D	30	Oven 15min
4	110	S	30	Oven 15min
5	55	S	30	Oven 15min
6	55	S	30	Oven 15min

When applying the optimized parameters for microporous glass on FTO glass, the result is nowhere near good. The substrate of FTO surface is not even fully covered. Some small adjustments were made, but still no good results can be obtained. Thus, it can be concluded that the spin coating parameters for microporous glass is totally different with FTO glass.

Using Vapor Method to Convert Lead Iodide

Besides electroplating, vapor conversion and chemical conversion were also tested. Chemical conversion is a method to put the substrate into a container of HI with a certain concentration and temperature. On the other hand, vapor conversion means using HI vapor to contact the lead dioxide layer, and then convert it to lead iodide.

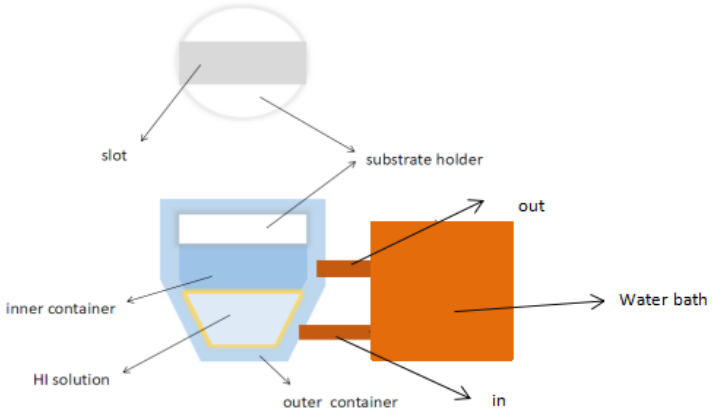

Fig. S3 Sketch of vapor deposition equipment.

Fig. S3 gives the sketch of the vapor conversion equipment. This equipment is consisting of one substrate holder and one double layer container. The holder is made of plastic which will not react with HI. Samples with lead dioxide facing down can be put on the slot, so that the vapor of HI solution would contact the lead dioxide film to trigger the conversion reaction.

The double layer container is a glass container with inner and outer vessels. The outer vessel can be filled with liquid from the pipes connected to it. One can use the lower pipe to fill water in and higher one to transport water out of the outer container. In this

experiment, this equipment is connected with a thermostatic water bath tank. Water with a certain temperature goes through the outer container and back to the tank in order to make the environment of the inner container possess a fixed temperature. By doing that, solution in inner container can evaporate with a steady speed.

Different temperature, concentration of HI and other parameters which may influence the outcome of the lead iodide film were studied in this thesis.

When fixing the volume of HI solution, and with the increasing of concentration, lead dioxide film would dissolve quicker. The speed of deposition cannot be correlated to HI concentration as a linear function because it is difficult to measure the deposition speed. Thus, other parameters should be considered to improve the quality of film.

Fig. S4 shows the illustration of substrate holder in Fig. S3 and all the trials used.

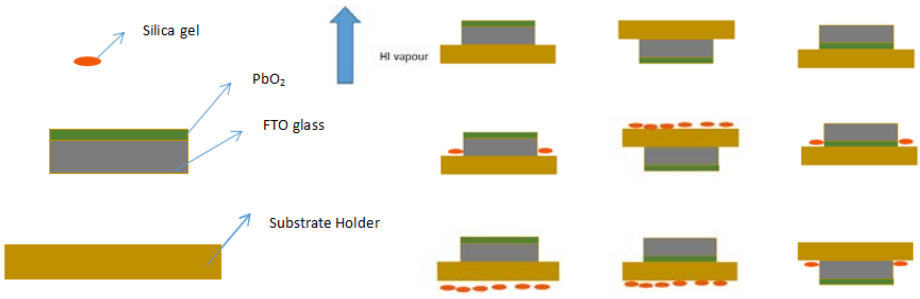

Fig. S4 Different trials used to explore Vapour deposition.

All the trials shown above showed non-uniform PbI_2 layers and poor conversion of the reactant.

Increasing the volume of solution, the total amount of HI increases. Also, the distance between substrate and solution phase would decrease. In this situation, the solution is less likely to evaporate as quickly as it does when have a smaller amount of HI solution. This decreases the speed of conversion. On the other hand, water vapor gathers around the surface of substrate. Small droplets formed and gradually become large ones. This would block the lead dioxide film from HI vapor which means no reaction could happen. The phenomena can also be seen when using water as solvent for HI.

Spin coating method is also tested to produce high quality lead iodide film. Different concentration of HI, speed of spin, volume of solution, mode of spin coating (dynamic or static) were studied.

A template with lead dioxide was put together with iodine in a sealed system at room temperature. Iodine can easily sublimate, and that makes the conversion of lead dioxide possible.

Manufacture conclusions

1. Plasma clean has to be as least 3 mins otherwise the surface obtained is not hydrophilic enough.
2. Plasma cleaned FTO glass is highly active, thus it needs to be used as soon as possible.
3. PEDOT: PSS solution need to be warm up before filter. The time for solution to reach 50℃ is different if with different containers. In this thesis, it is found that it takes bottles (10 ml volume) 30 mins to reach 50℃ in oven.
4. PEDOT: PSS should not be in the oven more than 120min, otherwise it will decompose and form other chemicals.
5. Thickness of PEDOT: PSS dose not influence the outcome of following lead dioxide, lead iodide and perovskite.
6. Using the same concentration mentioned in the thesis, solution for reference electrode calibration need to be changed every two days. Electrolyte for deposition need to be changed every 8 samples.
7. Keep lead dioxide coated samples in ethanol to protect the surface.
8. The chemical conversion of perovskite needs to be down in an environment with as less light as possible.